Engineered Science
DOI: https://dx.doi.org/10.30919/es1835

Research Advancements in Air Distribution Systems for Commercial Airliner Cabins in Recent Decades

Mingxin Liu,[1,*] Xingwang Zhao[2] and Yongzhi Zhang[3]

Abstract

With the outbreak of various influenza pandemics in recent years, the environment inside commercial airliner cabins has increasingly garnered attention. Enhancing the comfort of passengers and crew in airliner cabins, while simultaneously minimizing the risk of infectious disease transmission, has consistently been a focal point of scientific inquiry. An effective air distribution system is a pivotal factor in the quality of the airliner cabin environment. This paper examines pertinent articles dating back to 1992, particularly those that address air distribution systems in airliner cabins, ultimately about 120 articles were selected for review. These articles are categorized into four primary research areas: standards and guidelines pertaining to air distribution systems in airliner cabins, comparative analysis and synthesis of air distribution system research methods, comparative evaluation of various ventilation systems in airliner cabins, and innovative concepts for new air distribution systems in airliner cabins. The emergence of numerous innovative technologies and rapid technological advancements is evident in the frequent appearance of new articles, which contribute to the continual updating of knowledge. This review makes a significant contribution to the advancements in air distribution systems in airliner cabins and may prove beneficial to many scientists in this domain.

Keywords: Airliner cabins; Air distribution systems; Relative humidity; Air quality; Radiation air distribution system.

Received: 13 August 2025; Revised: 13 October 2025; Accepted: 15 October 2025.
Article type: Review article.

1. Introduction

According to the recent statistics from the International Air Transport Association, air transportation has emerged as an exceptionally favored mode of travel, exhibiting a consistent annual growth trend over the past five years.[1] After enduring extended periods of travel, an increasing number of passengers and crew have become more sensitive to the cabin environment.[2] Consequently, research into the internal airliner cabin environment is of paramount importance. Airliner cabin environment must fulfill the expectations of both passengers and crew members while also adhering to legal and technical requirements. A well-functioning environmental control system (ECS) on an aircraft can efficiently eliminate pollutants from the air, furnishing passengers and crew members with clean air and a comfortable airflow arrangement. To devise an improved ECS, it is imperative to delve into the characteristics of the air distribution system within airliner cabins. Air distribution systems are employed in airliner cabins to adjust the microclimate through technical controls.[3]

The air distribution systems in commercial airliner cabins are designed to regulate air temperature and velocity, while minimizing pollutant concentrations by ensuring adequate ventilation. The purpose of the air distribution system is to maintain the appropriate temperature and air quality inside the airliner cabins through air exchange, thereby fostering a thermally comfortable and secure environment for both passengers and crew.[3,4] Researches have shown that increasing the ventilation rate can effectively reduce the risk of infection spread by pathogenic microorganisms,[5] however, it may also result in a drafting sensation, causing thermal discomfort among passengers and crew. At this stage, extensive researches have been carried out in the area of air distribution systems in commercial airliners. Alongside improvements to traditional air distribution systems, researches have given rise to the development of numerous

[1] *School of Urban Construction, Changzhou University, Changzhou, 213164, China*
[2] *School of Energy and Environment, Southeast University, Nanjing, 210096, China*
[3] *College of Environmental Science and Engineering, Donghua University, Shanghai, 201620, China*
* *Email:* liumxczu@163.com (M. Liu)

innovative air distribution systems tailored for airliner cabins. However, despite these improvements, the systems still encounter numerous issues that impact the comfort and health of the airliner cabin environment. Addressing these concerns by effectively enhancing air quality and improving passenger thermal comfort remains a significant challenge in the operation of passenger airliner cabin ventilation systems.[6,7]

Since the comfort and safety of airliner cabins have been topics of public concern and discussion, research conducted by entities other than aircraft manufacturers has seen a substantial surge over the past decade. This research offers a meticulously crafted open database for all researchers involved in airliner cabin environmental issues, encompassing the characteristics of airliner cabin environments and research methodologies, thereby facilitating research and evidence gathering for relevant researchers.

The purpose of this paper was to analyze studies of ventilation systems in commercial airliner cabins since 1992. This objective was achieved through a literature review with a focus on four key issues: relevant standards for air distribution systems in airliner cabins, comparison and summary of research methods for air distribution systems, different types of air distribution systems, and innovative concepts for new air distribution systems in airliner cabins.

As part of the literature review, this paper analyzed scientific articles in the ScienceDirect and Web of Science databases. The search criteria included research articles, conference papers, and certain technical specifications published since 1992. Publications from other years that were considered crucial to a specific topic were also taken into account, ultimately enabling us to select about 120 articles for review.

2. Relevant standards and guidelines for air distribution systems in airliner cabins

This study collected and organized six sets of standards, guidelines, and regulations: three from the United States, two from Europe, and one from China, as outlined in Table 1.

Table 1 lists the requirements for air conditioning systems, control systems, and air quality across different regions inside airliner cabins. The specifications for air distribution systems encompass fresh air volume, circulating air volume, and total air volume. The requirements for control systems address both the cockpit and the passenger cabin. Meanwhile, air quality specifications include limits for CO, CO_2, O_3, particulate matter, and microorganisms. The temperature requirements for air distribution systems are also listed. According to ASHRAE Standard 161, the ambient temperature in airliner cabins should range from 18.3 °C to 23.9 °C and must not exceed 26.7 °C. The standard also defines horizontal and vertical temperature differences.

Regarding the air volume in airliner cabins, ASHRAE stipulates a minimum ventilation volume of 7.1 L/s per passenger,[8,9] with a recommended volume of 9.4 L/s per passenger. Moreover, the fresh air volume must not be less than 3.5 L/s per passenger. Because the safety-related humidity limit during flight is lower than the comfort threshold for passengers,[8] the relative humidity (RH) in the cabin was not explicitly specified in the regulations. Research has indicated that RH levels within the airliner cabin range from 15% to 35%.[10]

Bacteria, dust, and other substances tend to adhere more readily to the mucous membrane of the airway at low RH.[11-13] Meanwhile, moderately increasing the RH in airliner cabins can effectively reduce the occurrence of skin, eye, and nasal symptoms.[14] This phenomenon can be attributed to the decrease in the number of microorganisms in the air. Specifically, due to the superior tolerance of Gram-positive bacteria to dry conditions, the phenomenon may be linked to a reduction in the number of Gram-positive bacteria.[10] Therefore, some studies have suggested that RH in airliner cabins should not be excessively high, but should be maintained at approximately 30%.[10]

3. Research methods for air distribution systems in airliner cabins

Due to the large size of the airliner cabin and the difficulty of conducting experimental measurements during flight, general research has typically been conducted in ground-based experimental environmental mockups.[19] Generally, the focus of research on air distribution systems in airliner cabin mockups includes air distribution (velocity, temperature), along with pollutant concentration distribution. Research methods primarily fall into two categories: experimental measurement and numerical simulation. This paper provides a brief overview of the two methods.

Velocity measurement technology primarily encompasses single-point and full-field measurement instruments. Single-point velocity measurement technology comprises ultrasonic anemometry (UA),[2,20-24] hot bulb anemometry (HBA),[19] and hot-wire anemometry (HWA).[25] Table 2 provides information about single-point velocity measurement equipment. The benefits of single-point measurement technology include a wide velocity measurement range, flexible application, and simple operation. However, as instruments and equipment must be placed within the flow field, the measurement is intrusive and may affect the flow field. Hot bulb anemometers are typically employed to measure velocity under boundary conditions. Fig. S1 is a photograph of ultrasonic anemometers.

Full-field velocity measurement technology primarily encompasses particle image velocimetry (PIV),[20,26-29] particle tracking velocimetry (PTV),[30] and particle streak velocimetry (PSV).[31] PIV employs particle imaging technology, necessitating that a tracer gas be present at a high concentration and with a small particle size.[32] This method assumes that the tracer gas fully follows the airflow. When the motion of the particle swarm is captured at high speed with a camera and particle image analysis is performed, information about the flow field can be obtained. In addition, compared to the other two imaging techniques, PIV is the most widely used.

Table 1: Requirements for air distribution systems in airliner cabins.

Parameter	CCAR[15]	FAR[16]	BSEN 4618[17]	2019 ASHRAE HANDBOOK[9]	ASHRAE Standard 161-2023[8]	EASA[18]
Fresh air	0.55 pounds/min	0.55 pounds/min	-	3.5 L/s per passenger (fresh air)	3.5 L/s per passenger (fresh air)	0.55 pounds/min
Recirculated air	-	-	-	4.7 L/s per person (recirculated air)	-	-
Total air	-	-	-	9.4 L/s per person (total air)	9.4 L/s per person (total air)	-
Hazardous gas threshold	1)CO 50 ppm 2)CO_2 5,000 ppm 3)O_3 0.25 ppm (any time above flight level 320) 4)O_3 0.1 ppm (any 3-hour interval above flight level 270)	1)CO 50 ppm 2)CO_2 5,000 ppm 3)O_3 0.25 ppm (any time above flight level 320 4)O_3 0.1 ppm (any 3-hour interval above flight level 270)	1)CO 50 ppm (safety); CO 25 ppm (TWA 1 h), 10 ppm (TWA 8 h) (health) 2)CO_2 5,000 ppm (safety); CO_2 2,000 ppm (health); CO_2 2,000 ppm (comfort); 3)O_3 0.25 ppm (any time above flight level 320) 4)O_3 0.1 ppm (any 3-hour interval above flight level 270) 5)Ultrafine particle: 100,000-300,000 particles/cm^3 (during taxiing) 500 particles/cm^3 (during cruising) 6)PM 2.5: 100 µg.m^3 (TWA 1 h) 40 µg.m^3 (continuous) 7)PM 10: 150 µg.m^3 (TWA 24 h) 8)Micro-organisms ≤ 500 cfu.m^3 (by ventilation, 24 h)	1)CO 50 ppm 2)CO_2 5,000 ppm 3)O_3 0.25 ppm (any time above flight level 320) 4) O_3 0.1 ppm (any 3-hour interval above flight level 270)	1)O_3 0.25 ppm (any time above flight level 320) 2)O_3 0.1 ppm (any 3-hour interval above flight level 270)	1)CO 50 ppm 2)CO_2 5,000 ppm 3)O_3 0.25 ppm (any time above flight level 320) 4)O_3 0.1 ppm (any 3-hour interval above flight level 270)
Thermal comfort and thermal satisfaction			Draft risk (DR) <15%; − 0.7 < PMV < 0.7			
Cockpit requirements	Smoke evacuation must be readily accomplished, starting with full pressurization and without depressurizing beyond safe limits.	Smoke evacuation must be readily accomplished, starting with full pressurization and without depressurizing beyond safe limits.				Smoke evacuation must be readily accomplished, starting with full pressurization and without depressurizing beyond safe limits.

Parameter	CCAR [15]	FAR [16]	BSEN 4618 [17]	2019 ASHRAE HANDBOOK [9]	ASHRAE Standard 161-2023 [8]	EASA [18]
Cockpit area	1)The temperature and quantity of air supplied can be controlled independently. 2)The air inlets and passages for air to flow between flight crew and passenger compartments are arranged to provide compartment temperatures within 3 °C.	1)The temperature and quantity of air supplied can be controlled independently. 2)The air inlets and passages for air to flow between flight crew and passenger compartments are arranged to provide compartment temperatures within 3 °C.				1)The temperature and quantity of air supplied can be controlled independently. 2)The air inlets and passages for air to flow between flight crew and passenger compartments are arranged to provide compartment temperatures within 2.8 °C.
Cabin temperature			Vertical temperature gradient 3.5 °C/m (0.1 m to 1.1 m height)		1)Target operative temperature range in-flight and during ground operations: 18.3 °C to 23.9 °C; 2)Operative temperature in flight shall not exceed 26.7 °C; 3)Horizontal operative temperature variation across each temperature control zone: <4.4 °C 4)Vertical operative temperature variation within a seat (seat centerline): <2.8 °C	

Note:

1) TWA stands for time-weighted average;

2) Safety limits: limits for cabin environment parameters that if exceeded would prevent the safe operation of the aircraft;

3) Health limits: limits for cabin environment parameters that if exceeded would lead to temporary or permanent pathological effects on the occupants;

4) Comfort limits: limits for cabin environment parameters that if exceeded would not provide an acceptable cabin environment.

Table 2: Information about single-point velocity measurement instruments.

Instrument	Sampling frequency	Measurement range	Resolution	Accuracy
Ultrasonic anemometer	20 Hz	0–10 m/s	0.005 m/s	±1%
Hot-sphere anemometer	8 Hz	0.05–5 m/s	0.01 m/s	±1 – ±5 %
Hot-wire anemometry	—	0–30 m/s	0.01 m/s	±3%

Meanwhile, the PTV technique obtains flow field information by tracking the motion of individual particles. PTV requires a low concentration of tracer particles and a larger particle size, facilitating easy tracking. This method can yield more precise flow field data in low-speed environments. PSV, on the other hand, tracks the movement trajectories of particles to gather flow field information. This technique again involves tracer particles at a low concentration and a larger particle size. Both PTV and PSV are primarily utilized in low-speed flow fields. The advantage of full-field velocity measurement technology lies in its ability to capture comprehensive flow information. Additionally, its embedded measurement method is non-contact, ensuring that there is no impact on the flow field and providing high spatial resolution.[33] However, since full-field velocity measurement technology requires laser irradiation, there cannot be any obstructions in the light path or field of view. Even with full-field measurement, the single measurement range remains quite limited. For large-scale flow fields, stitching is necessary. Furthermore, the technology is expensive, and the operation is relatively complex. Fig. 1 displays a schematic diagram of PIV flow field testing in a cabin mockup.

Twenty-four global flow field tests in airliner cabins were conducted from 1992 to 2021, as detailed in Table 3. These studies were distributed across the United States, Germany, and China. The primary research methods employed were UAs, PTV and PIV, with experimental scopes ranging from a small section of a cabin to an entire large section. Due to the low air velocity within airliner cabins, PIV velocimetry technology or ultrasonic anemometers (UAs) were commonly employed in the experiments.[34-36] PIV measurement can yield high-resolution data,[37-39] but the measurements were constrained by obstacles, such as seats and dummies; thus, air distribution could only be obtained in the upper part of the airliner cabin.[40,41] Ultrasonic anemometers have a high measurement frequency, enabling the acquisition of high-quality three-dimensional air distribution data around dummies. In recent years, experimental research has primarily focused on UAs and PIV, examining one or several large sections.

The accuracy of single-point velocity measurement is highly dependent on the sampling size and location.[42,43] The sampling size refers to the number of sampling locations, while the sampling location refers to the specific place where sampling occurs. To minimize measurement time and labor costs, the sampling size should be reduced. However, having too few sampling points may lead to low spatial resolution.[43] Studies have indicated that when UAs with a resolution of 150 mm × 150 mm are used, the measurement results closely align with the actual flow field.[44] The latest flow field studies (UAS) in airliner cabins were all conducted based on this resolution.[19,45,46]

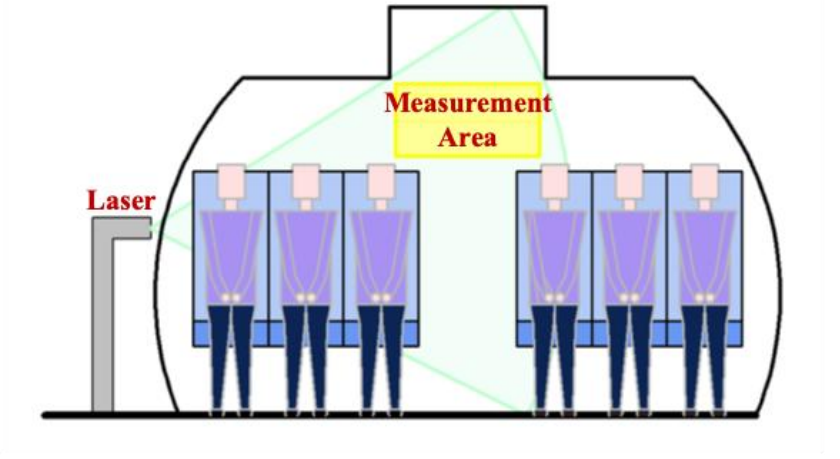

Fig. 1: Schematic of a 2D–2C PIV measurement system.

Simultaneously, researchers monitored the designated point for up to 60 minutes and discovered that the time-averaged value over a 4-minute measurement period was essentially similar to that over a 60-minute period, with an error margin of less than 10%,[47-49] as detailed in Fig. 2. In addition, existing research have shown that a certain waiting time is required before each data measurement to ensure the stability of the air distribution.[48,50] Generally, the waiting time is not less than 3 minutes.

To shorten the measurement cycle and minimize the interference caused by personnel moving measurement points, some studies utilized 3D robotic systems to drive measuring instruments for precise fixed-point measurements.[19,48,51,52] The positioning accuracy of these robots can reach ±0.05 mm. To calibrate the impact of positioning robots on the flow field, researchers conducted velocity measurements at specific points.[48] Calibration was divided into two scenarios: when the 3D robot was approaching the measurement point and when it was moving away from it.[48] The results indicated that the relative deviation of the average velocity between the two operating conditions is within 7%, and the relative deviation of turbulence intensity is within 4%.[48] Therefore, the impact of the 3D robot on the flow field can be neglected.

Additionally, leveraging the characteristics of UAs and PIV, some scholars have proposed a combination of these two experimental methods for the sake of higher-precision data.[45] However, this combined experimental approach demands a high level of transparency for cabin mockups, necessitating either full or partial transparency in its design.

3.1.2 Measurement methods for pollutant concentration distributions

The distribution of pollutants in airliner cabins impacts air quality and poses a threat to the health of passengers and crew. Therefore, it is imperative to investigate the patterns of pollutant distribution within airliner cabins. Generally, gaseous pollutants or particles have been used for this purpose.

(1) Gaseous pollutant: Since small particles are able to closely follow airflow, some studies have utilized gaseous pollutants as proxies for fine particles. Common tracer gases used to simulate gaseous pollutants include CO_2,[20,56] and mixed sulfur hexafluoride (SF_6) (1% SF_6, 99% N_2).[2,45] However, the concentration of CO_2 can be influenced by the background environment and operators, whereas SF_6, which is non-toxic, stable, and easy to detect, is present in very low concentrations in the background environment. Therefore, most studies have opted for SF_6 as the simulated pollutant. Typically, the concentration distribution of SF_6 has been analyzed using an infrared photoacoustic gas analyzer (INNOVA 1412).

(2) Particle concentration: To investigate the spread of infectious diseases within airliner cabins, it is imperative to study the distribution of particulate matter. In particle distribution research, both particle size and quantity have played a crucial role in determining experimental outcomes. Typically, infectious diseases are caused by viruses and bacteria. Studies have indicated that viruses typically have a diameter of less than 0.1 μm,[61] and often reside on bacteria ranging from 0.2 to 3.2 μm for transmission,[62] whereas most bacteria measure between 0.4 and 10 μm in diameter.[61] Furthermore, particles with an aerodynamic diameter below 1.0 μm exhibit similar propagation patterns to those of gaseous pollutants,[63] while particles larger than 5 μm settle rapidly in the air.[64]

Both mass concentration and count concentration can be used to represent particulate matter concentration in measurements.[65] Particle mass concentration refers to the total mass of particulate matter contained within a unit volume of air.[66] It has typically been used to quantify the content of total particulate matter in the air, such as $PM_{2.5}$ or PM_{10}. The primary measurement methods include the weighing method,

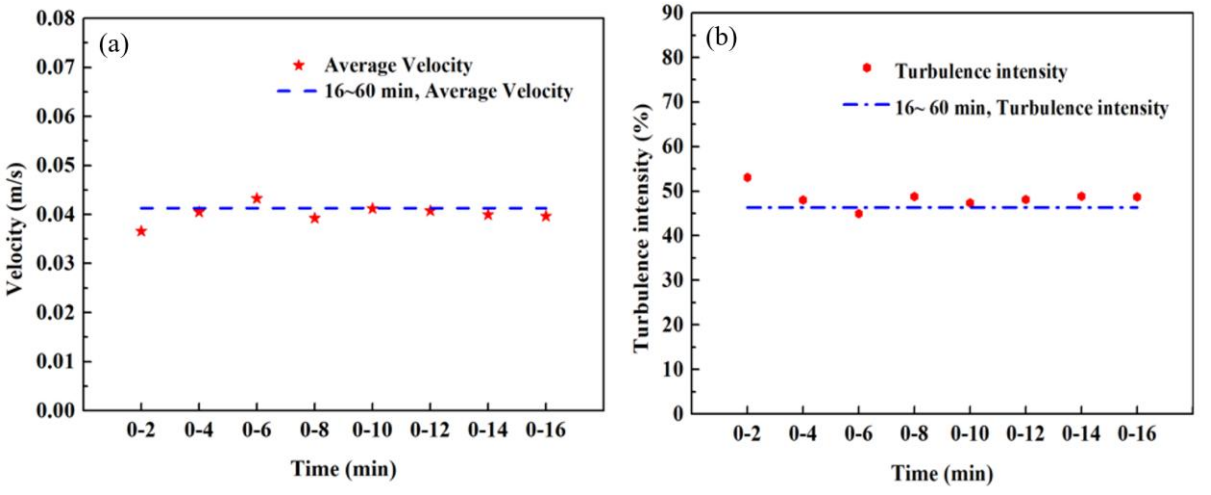

Fig. 2: Compare the average wind speed (a) and turbulence intensity (b) during different time periods (Data sourced from reference).[47]

Table 3: Requirements for ventilation systems in airliner cabins.

Serial number	Research unit	Year	Experimental platform	In-cabin conditions	Experimental method	Measurement range
1	The Boeing Company[53]	1992	Simplified cabin mockup	Unoccupied	HWA	Half cross-section (43 × 2 points)
2	Airbus[26]	1997	A340 mockup	Unoccupied	PTV (helium bubble)	Half cross-section (above the seat)
3	The Boeing Company[54]	2002	Simplified cabin mockup	Occupied	PIV (DEHS)	One cross-section
4	Federal Aviation Administration[22]	2003	B747 mockup	Empty	UA	One cross-section (40 points)
5	Kansas State University[55]	2003	B737 mockup	Occupied	PIV	Three small areas
6	The Boeing Company[25]	2005	B767 mockup	Occupied	HWA	Five points
7	The Boeing Company[30]	2006	Simplified cabin mockup	Empty	PIV (plastic pellet)	Five small areas (0.36 m x 0.36 m)
8	German Aerospace Center[27]	2006	A380 mockup	Empty	PIV (helium bubble)	Half cross-section
9	German Aerospace Center[28]	2006	A380 mockup	Empty	PIV (DEHS)	Luggage rack wall area
10	University of Illinois[56]	2008	B767 mockup	Occupied	PTV (helium bubble)	Half cross-section (above a dummy's head)
11	Purdue University[57]	2008	B767 mockup	Occupied	PIV	Six small areas
12	University of Illinois at Urbana-Champaign[56]	2008	B767 mockup	Occupied	PTV	One large area
13	DLR[58]	2009	A380 mockup	Occupied	PIV (helium bubble)	Half cross-section
14	Purdue University[2]	2009	B767 mockup	Occupied	UA	Cross-section and longitudinal section (103 points)
15	Hong Kong University of Science and Technology[29]	2009	Simplified cabin mockup	Occupied	PIV (DEHS)	Five small areas (210 mm × 158 mm)
16	German Aerospace Center[41]	2009	A380 mockup	Occupied	PIV	One large area
17	Hamburg University of Technology[59]	2010	Full-scale cabin mock-up	Occupied	PIV	Two small areas
18	Purdue University[38]	2010	Small-scale, water-filled model	Empty	PIV	Two small areas
19	Dalian University of Technology[20]	2012	B767 mockup	Occupied	UAs	One cross-section (83 points); one longitudinal section (42 points)
20	Tianjin University[21]	2012	MD-82 first-class cabin	Unoccupied	UAs	Three cross-sections (343 points per cross-section)
21	Institute of Aerodynamics and Flow Technology[60]	2013	Do 728	Occupied	PIV (DEHS)	Two small areas
22	Tianjin University[23]	2013	MD-82 first-class cabin	Occupied	UAs	Three longitudinal sections (304 points per section)

Serial number	Research unit	Year	Experimental platform	In-cabin conditions	Experimental method	Measurement range
23	Tianjin University[37]	2015	Full-size seven row cabin mockup	Occupied	PIV (DEHS)	Three cross-sections, one longitudinal section, and one horizontal section
24	Tianjin University[19]	2021	Full-size seven-row cabin mockup	Occupied	UAs	One cross-section, one longitudinal section

Note: 1) DEHS is Di-Ethyl-Hexyl-Sebacat; 2) helium filled soap bubbles (HFSB).

oscillating balance method, and beta ray method. The particle count concentration denotes the total number of particles per unit volume of air. The concentration of particulate matter in airliner cabins is commonly characterized in terms of particle count concentration, which is generally used to assess the risk of infectious disease transmission.[29] The instruments commonly used to measure particle count concentration, along with the characteristics of these instruments, are shown in Table 4.

Early studies primarily focused on measuring the concentration of particulate matter at representative scatter points inside the cabin.[67,68] Scatter point measurements enabled the assessment of hourly concentration changes of particulate matter at specific points inside the cabin, or the average concentration at that location. As measurement efficiency improves, an increasing number of are now measuring the particulate matter concentration fields within main cross-sections.[69] This measurement approach enables a clearer assessment of the distribution and spatial propagation path of particulate matter content within the space. According to the verification protocol for Computational Fluid Dynamics (CFD) calculation programs recommended by ASHRAE,[70] utilizing the results of particle concentration field measurements in the main sections to validate CFD simulation results can enhance the persuasiveness of the verification process.

Both monodisperse particle sources and polydisperse particle sources have commonly been used to generate particles in experimental studies.[51,71] Monodisperse particle generators can release particles within a narrow size range, whereas polydisperse particle generators can release particles ranging from 0.5 to 10 μm in diameter. During the experiments, the requirement was that the average concentration of particulate matter released in the chamber should be least 2 orders of magnitude higher than the background concentration prior to the release of the particle source.[51] Plant oil and DEHS oil have commonly been employed as dust-generating oils.[72,73] The physical properties of plant oil and DEHS oil are not significantly different. They are distinguished primarily by their densities: plant oil has a density of 0.917 g/mL, whereas DEHS oil has a density of 0.912 g/mL. Plant oil is less thermally stable than DEHS, potentially leading to particle size evolution of the former due to oil evaporation. The measurement results indicated that the concentration distributions obtained using the two types of oils were remarkably similar. However, when plant oil was used as the dust source, the diffusion range was found to be larger than that of DEHS, whereas when DEHS was used as the dust source, the experimental results were more stable.

Table 4: Particle concentration field measurement instruments.

Instrument	Model	Measurement range	Characteristics
Particle counter	TSI 9310/9510	There are 6 channels (TSI 9310) within the particle size range of 0.3–25 μm and 6 channels (TSI 9510) within the particle size range of 0.5–25 μm.	The number of particle channels is limited, and the statistical range of particle size is broad, resulting in low accuracy.
Aerosol particle size spectrometer	TSI 3321	There are 52 channels within the particle size range of 0.5–20 μm.	The number of particle channels is significantly high, and the statistical range of particle size is narrow, resulting in high accuracy.

To minimize the interference of particulate matter release sources on the flow field in cabin mockups, the outflow velocity of particles at the release source should be minimized. When the momentum of particle release is reduced, particles can be released more uniformly at the source.[69] When the particle release velocity is much lower than the flow velocity in the surrounding environment, it can be considered that there is no momentum release from the particulate matter release source. Fig. S2 illustrates the particulate matter release source in a certain experimental process. This release source was a porous acrylic bead with a diameter of 8 cm and with 400 small holes (3 mm in diameter) uniformly distributed across its surface for releasing particulate matter.[51] Additionally, the bead was filled with cotton to achieve the purpose of releasing particulate matter without momentum.

In the processing of raw data, if comparison with simulation results is required, data normalization is necessary. Specifically, the nominal fully mixed concentration, also known as the nominal exhaust duct concentration without considering particle transmission loss, is calculated using the release amount of pollution sources in the cabin and the air supply volume to the cabin. Subsequently, the ratio is obtained by subtracting the background concentration in cabin mockups from both the measured average value at each point and the nominal fully mixed exhaust duct concentration. Detailed calculations are performed by means of Eqs. (1) and (2).

$$C = \frac{C_{local} - C_{in}}{C_{out} - C_{in}} \quad (1)$$

where C_{local} is the particle number concentration at a sampling point, particles/cm^3; C_{in} is the particle number concentration in the air supply, particles/cm^3; and C_{out} is the nominal exhaust particle concentration without considering particle transmission loss, particles/cm^3.

$$C_{out} = \frac{Q_{source} \times C_{source}}{Q_{ventilation}} \quad (2)$$

where Q_{source} is the particle-laden gas flow rate from a single release source, L/min; C_{source} is the number concentration of the particle source, particles/cm^3; and $Q_{ventilation}$ is the total air-supply rate into the cabin, m^3/h.

3.2 Numerical simulation

3.2.1 Numerical simulation of air distributions

Although the experimental measurement method is highly accurate, it is costly and time-consuming. Computational fluid dynamics (CFD) provides more detailed information and significantly reduces time and labor costs, making it a widely used method in studies of airliner cabin air distribution systems.[74] Commonly used CFD simulation tools include STAR-CCM, CFX, ANSYS Fluent, and Open-FOAM. To date, ANSYS Fluent has the highest utilization rate. Generally, there are three main CFD simulation methods: direct numerical simulation (DNS), large-eddy simulation (LES), and Reynolds-averaged Navier-Stokes (RANS) models.[23,75,76] The characteristics of these simulation methods are detailed in Table 5. The published research findings have indicated that RANS models are the preferred method due to their relatively low computer performance requirements and swift calculations. RANS models encompass the standard k-ε model, the RNG k-ε model, the realizable k-ε model, and the SST k-ω model.[77]

Cao *et al*. were the first to systematically investigate the disparities between these two-equation RANS models and experimental measurements in predicting airflow distribution within cabin mockups. They simulated and trained the four turbulence models, as illustrated in Figs. 3 and 4. According to their findings, the realizable k-ε model is the turbulence

Table 5: Characteristics of different CFD simulation methods.

Simulation method	Characteristics
DNS	Numerical problems are directly solved by means of control equations without the need for turbulence modeling; It is necessary to obtain flow information for multi-scale turbulence, which requires high spatial and temporal resolution; The method is time-consuming, computationally intensive, and heavily reliant on computer memory; Generally, calculations can only be performed for simple turbulent motions with low Reynolds numbers, and are not suitable for complex turbulent flows inside the cabin.
LES	First, vortices of different scales are separated, and the large-scale vortices are directly simulated while the small-scale vortices are enclosed by the model; The degree of computational complexity is between that of DNS and RANS; Although the computational load is relatively small compared to DNS, the computer's memory requirement is high and the computation cycle is long;
RANS	The governing equation is the Navier-Stokes (N-S) equation; Based on Boussinesq's hypothesis, turbulent Reynolds stress is directly proportional to strain, and is calculated using the proportionality coefficient; The method demands minimal computer memory and boasts relatively short computation cycles; It is commonly employed for simulation of airliner cabin flow fields.

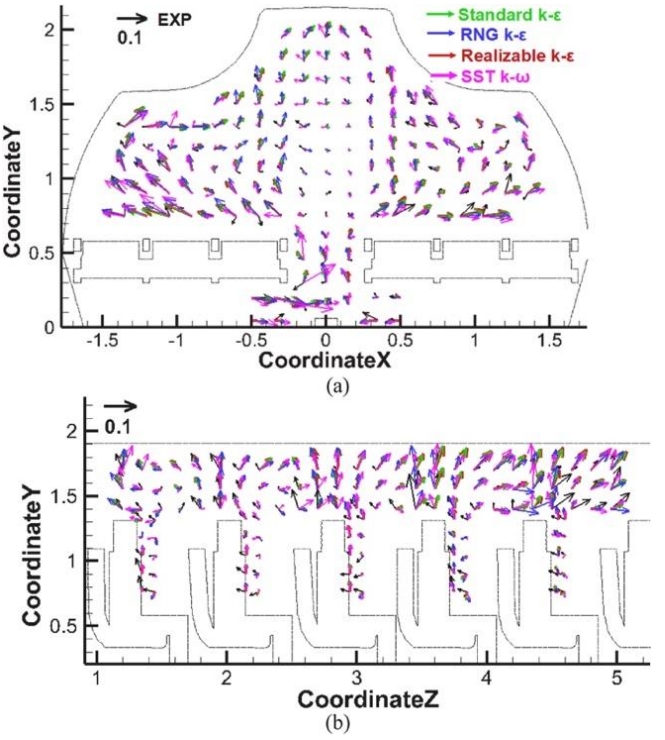

Fig. 3: Qualitative comparison of velocity fields predicted by different turbulence models in (a) a cross section and (b) a longitudinal section.[78]

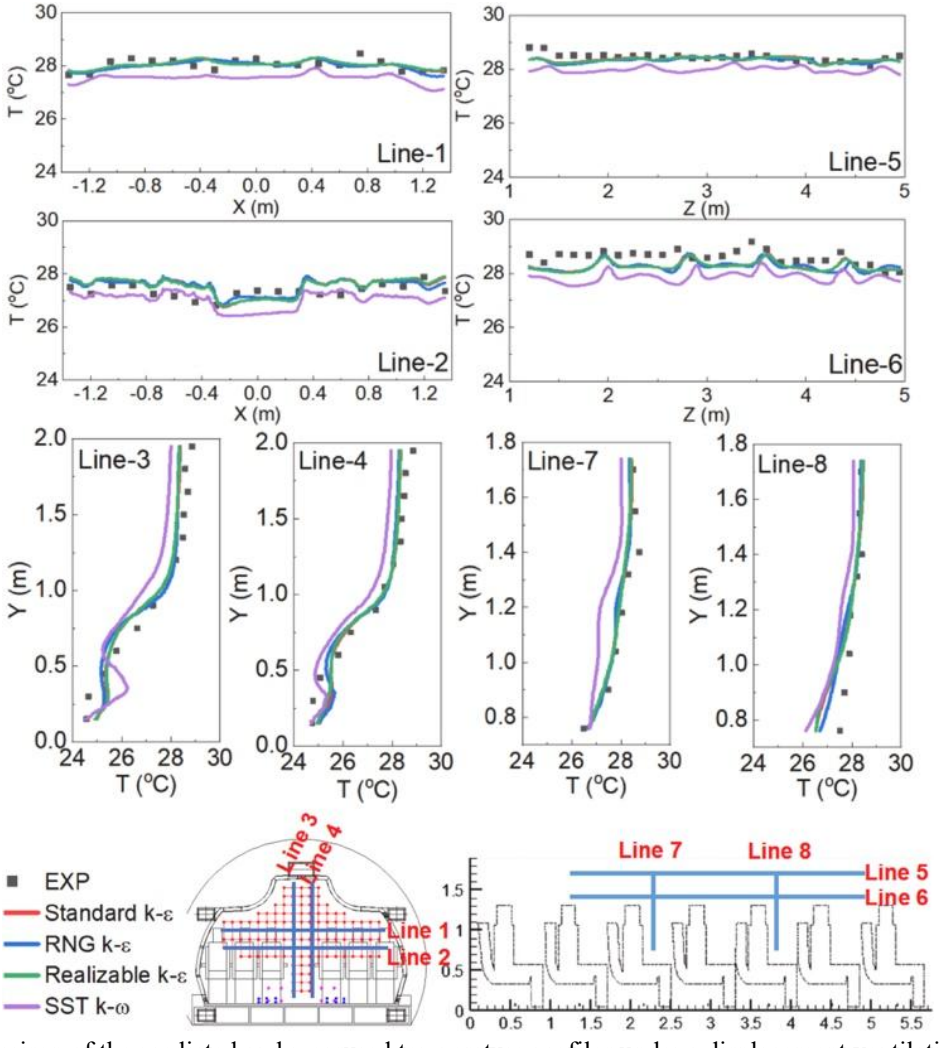

Fig. 4: Comparison of the predicted and measured temperature profiles under a displacement ventilation system.[78]

model that most closely matches the experimental values,[78] as presented in Table 6. The unified expression for these three turbulence models is given in Eq. (3):

$$\rho\frac{\partial\bar{\Phi}}{\partial t}+\rho\bar{u}_i\frac{\partial\bar{\Phi}}{\partial x_i}-\frac{\partial}{\partial x_i}\left[\Gamma_{\phi,eff}\frac{\partial\bar{\Phi}}{\partial x_i}\right]=S_\phi \quad (3)$$

where ϕ represents the flow variables, $\Gamma_{\phi,eff}$ the effective diffusion coefficient, and S_ϕ the source term. Table 7 presents the general forms that can be used to describe the four turbulence models.

Currently, in airliner cabin studies, grid size is determined using the grid-independent solution method in large-scale simulations, yet there is no specific regulation for local grid size. Some studies, however, have provided a more detailed specification for the grid size based on turbulence scales in airliner cabin ventilation simulation research. To analyze the temporal and spatial characteristics of turbulence, the integral scale, Kolmogorov scale, and Taylor scale can be used. The integral scale characterizes the largest vortex; the Kolmogorov scale represents the dissipation scale; and the Taylor scale delineates the smallest discernible vortex. Additionally, spatial-temporal scales can be interconverted, as proposed in Taylor's "frozen turbulence" hypothesis.[79] The calculation formulas for turbulence scale are shown in Eqs. (4)-(9).

$$Its=\int_0^{+\infty}f(\tau)\,d\tau,\ f(\tau)=\frac{V(t)V(t+\tau)}{V(t)^2} \quad (4)$$

$$Iss=Its\times\bar{V} \quad (5)$$

$$Tts=[-f''(0)]^{1/2} \quad (6)$$

$$Tss=\langle V^2\rangle^{1/2}/\langle(\partial V/\partial x)^2\rangle^{1/2},\ \frac{\partial V}{\partial x}=-\frac{1}{V}\times\frac{\partial V}{\partial\tau} \quad (7)$$

$$Dts=(\nu/\varepsilon)^{1/2} \quad (8)$$

$$Dss=(\nu^3/\langle\varepsilon\rangle)^{1/4},\ \langle\varepsilon\rangle=15\nu\langle(\partial V/\partial x)^2\rangle \quad (9)$$

where *Its* is the integral temporal scale (s); *Iss* is the integral spatial scale (m); *Tts* is the Taylor temporal scale (s); *Tss* is the Taylor spatial scale (m); *Dts* is the Kolmogorov temporal scale (s); *Dss* is the Kolmogorov spatial scale (m); $f(\tau)$ is the time autocorrelation function; τ,t is time (s); and $\langle\varepsilon\rangle$ is the mean dissipation rate.

Table 6: Averaged quantitative deviation of modeling results predicted by different turbulence models and measured data.[78]

Turbulence models	Averaged absolute error of velocity (m/s)	Averaged relative error of velocity (%)	Averaged absolute error of temperature (°C)	Averaged relative error of temperature (%)
Standard k-ε	0.019	52.20	0.300	1.08
RNG k-ε	0.022	60.46	0.301	1.08
Realizable k-ε	0.019	52.12	0.295	1.07
SST k-ω	0.024	63.23	0.548	1.96

Table 7: Coefficients and source terms for the governing equations.[78]

		ϕ	$\Gamma_{\phi,eff}$	S_ϕ	Constants
Reynolds-averaged variables	Continuity	1	0		
	Momentum	u_j	$\mu+\mu_t$	$-\frac{\partial p}{\partial x_i}+\frac{\partial}{\partial x_j}\left[(\mu+\mu_t)\frac{\partial u_j}{\partial x_i}\right]$	
	Temperature	T	$\frac{\mu}{Pr}+\frac{\mu_t}{\sigma_T}$	S_T	
Standard k-ε		k	$\mu+\frac{\mu_t}{\sigma_k}$	$G_k+G_b-\rho\varepsilon$	$\mu_t=\rho C_\mu\frac{k^2}{\varepsilon}$, $G_K=\mu_t S^2$, $S=\sqrt{2S_{ij}S_{ij}}$, σ_ε=1.3, C_μ=0.09, $G_b=\beta g_i\frac{\partial\mu_t}{\partial\sigma_{T,t}}\frac{\partial\bar{T}}{\partial x_i}$, $C_{1,\varepsilon}$=1.44, $C_{2,\varepsilon}$=1.92, σ_k=1.0,
		ε	$\mu+\frac{\mu_t}{\sigma_\varepsilon}$	$C_{1\varepsilon}G_k\frac{\varepsilon}{k}-C_{2\varepsilon}\rho\frac{\varepsilon^2}{k}$	
RNG k-ε		k	$\mu+\frac{\mu_t}{\sigma_k}$	$G_k+G_b-\rho\varepsilon$	$\mu_t=\rho C_\mu\frac{k^2}{\varepsilon}$, $G_K=\mu_t S^2$, $S=\sqrt{2S_{ij}S_{ij}}$, $G_b=\beta g_i\frac{\partial\mu_t}{\partial\sigma_{T,t}}\frac{\partial\bar{T}}{\partial x_i}$, $R_\varepsilon=\frac{C_\mu\rho\eta^3(1-\eta/\eta_0)}{1+\beta\eta^3}\frac{\varepsilon^2}{k}$, $\eta=Sk/\varepsilon$, η_0=4.38, β=0.012, σ_k=1.0, σ_ε=1.3, C_μ=0.0845, $C_{1,\varepsilon}$=1.42, $C_{2,\varepsilon}$=1.68
		ε	$\mu+\frac{\mu_t}{\sigma_\varepsilon}$	$C_{1\varepsilon}G_k\frac{\varepsilon}{k}-C_{2\varepsilon}\rho\frac{\varepsilon^2}{k}-R_\varepsilon$	
Realizable k-ε		k	$\mu+\frac{\mu_t}{\sigma_k}$	$G_k+G_b-\rho\varepsilon$	$\mu_t=\rho C_\mu\frac{k^2}{\varepsilon}$, $G_k=\mu_t S^2$, $S=\sqrt{2S_{ij}S_{ij}}$, $G_b=\beta g_i\frac{\partial\mu_t}{\partial\sigma_{T,t}}\frac{\partial\bar{T}}{\partial x_i}$, $\eta=Sk/\varepsilon$, $C_1=max\left[0.43,\frac{\eta}{\eta+5}\right]$, C_2=1.9, $C_{1,\varepsilon}$=1.44, $C_\mu=\frac{1}{A_0+A_s(kU^*/\varepsilon)}$, $U^*\equiv\sqrt{S_{ij}S_{ij}+\widetilde{\Omega}_{ij}\widetilde{\Omega}_{ij}}$, σ_k=1.0, σ_ε=1.2, $\mu_t=\frac{\rho k}{\omega}\frac{1}{max[(1/\alpha^*),SF_2/a_1\omega]}$, $\sigma_k=\frac{1}{\frac{F_1}{\sigma_{k,1}}+\frac{(1-F_1)}{\sigma_{k,2}}}$, $\sigma_\omega=\frac{1}{\frac{F_1}{\sigma_{\omega,1}}+\frac{(1-F_1)}{\sigma_{\omega,2}}}$,
		ε	$\mu+\frac{\mu_t}{\sigma_\varepsilon}$	$\rho C_1S_\varepsilon-\rho C_2\frac{\varepsilon^2}{k+\sqrt{\nu\varepsilon}}$	
SST k-ω		k	$\mu+\frac{\mu_t}{\sigma_k}$	G_k-Y_k	$G_k=\mu_t S^2$, $G_\omega=\frac{\alpha}{\nu_t}\widetilde{G}_k$, $\widetilde{G}_k=min\left(G_k,10\rho\beta^*k\omega\right)$, $Y_k=\rho\beta^*k\omega$, $Y_\omega=\rho\beta\omega^2$, $\sigma_{k,1}$=1.176, $\sigma_{\omega,1}$=2.0, $\sigma_{k,2}$=1.0, $\sigma_{\omega,2}$=1.168, a_1=0.31

The grid size can be guided by the size distribution of the vortex in CFD. DNS requires the simulation of full-scale turbulence, and the grid size should be smaller than the Kolmogorov space scale. The RANS equation establishes the model for Reynolds stress caused by velocity fluctuations on all scales, and the grid size should be larger than the integral space scale. The grid resolution of LES falls between that of DNS and RANS, with the grid length being identical to the inertial subscale.[80] Table 8 shows the grid scales for different models in different locations.[81,82] Currently, the recommendations for grid size settings are not comprehensive, and certain aspects remained unexplored.

3.2.2 Numerical simulation of pollutant concentration distributions

According to the literature on CFD simulation and calculation of pollutant distributions in commercial airliner cabins, the Lagrangian and Eulerian methods have become very popular in recent years for simulation and calculation of pollutant transport. The Eulerian method treats pollutants as a continuous phase, considering them as a phase in the air, and solves their mass transfer equations. The pollutants can be treated as a continuous phase because their size is significantly smaller than the Kolmogorow size in the flow field. Second, the volume ratio of the releaed particles is much smaller than 10:6, and thus is below the threshold for considering their reaction to airflow.[83] The Lagrangian method analyzes the force exerted on each particle and calculates their trajectories. In this approach, particles are treated as discrete phases. Since the Lagrangian model can obtain the motion trajectory of each particle, it allows us to understand the "destiny" of particles in the computational environment. Furthermore, when the trajectories of a sufficient number of particles are calculated, a "continuous" concentration field can be obtained. The accuracy of both the Eulerian method and the Lagrangian method in calculating the distribution of indoor pollutant concentrations has been verified experimentally. The calculation methods for pollutant concentration in the retrieved literature are summarized in Table 9

Table 8: Grid scales for different models.

Location	Ventilation type	DNS	LES	RANS
		< Dss	Dss < GS < Iss	Iss ≤ GS < L
Aisle[81]	Mixing ventilation	0.3 mm	0.3–100 mm	100 mm
Above dummies[82]	Mixing ventilation	0.8 mm	0.8–40 mm	40 mm
	Displacement ventilation	0.6 mm	0.6–1 mm	1 mm

Table 9: Summary of calculation methods for pollutant concentration in literature retrieval.[78,84]

Calculation method for particle concentration	Governing equation	Coefficients
Eulerian method	$\frac{\partial \rho C}{\partial t}+\frac{\partial}{\partial x_i}\left(\rho\left(\bar{u}_i+\overrightarrow{V_{Si}}\right)C-\Gamma\frac{\partial C}{\partial x_i}\right)=S_C$	$\Gamma=\rho\left(D+v_p\right)$ $V_s=\frac{\rho_p d_p^2 g C_c}{18\mu_a}$ $C_c=1+\frac{2\lambda}{d_p}(1.257+0.4exp(-1.1d_p/2\lambda))$
Lagrangian method	$\frac{d\vec{u}_p}{dt}=F_D(\vec{u}-\vec{u}_p)+\frac{\vec{g}(\rho_P-\rho)}{\rho_P}+\vec{F}_a$	$u_i^{'}=\zeta\sqrt{2k/3}$ $C_j=\frac{\dot{M}\sum_{i=1}^{m} dt_{(i,j)}}{V_j}$

Note: 1) where t is time, C the particle concentration, ρ the density of air, $x_i(i=1,2,3)$ the three coordinates, $\bar{u}_i$ the averaged air velocity components in the three directions, Γ the effective particle diffusivity, S_C the generation rate of the particle source, and $\overrightarrow{V_S}$ the settling velocity of particles. 2) where D is the Brownian diffusivity of particles, and v_p the particle turbulent diffusion coefficient. When particle size is larger than 0.01 μm, the Brownian diffusivity may be negligible compared with turbulent diffusivity in a turbulent flow. The relationship between the particle turbulent diffusion coefficient v_p and the gas diffusion coefficient v_t has been theoretically studied by Tchen;[86] Hinze then developed a mathematical derivation of their relationship.[87] It can be stated that when the Stokes number of a particle approaches zero in a homogeneous turbulent flow, v_p is equal to v_t. Although real airflows may not satisfy the homogeneous assumption used in the theory, this equality still holds as long as the Stokes number of particles remains low.[88] 3) where ρ_p is the particle density, d_p the particle diameter, μ_a the air viscosity, g the gravitational acceleration, and C_c the Cunningham correction factor. 4) where λ is the mean free path of air molecules, which is 0.066 μm when the air temperature is 20 °C and pressure is 0.1 Mpa. 5) where $\vec{u}_p$ is the particle velocity vector, F_D the inverse of relaxation time, and $\vec{u}$ the air velocity; the second term represents the gravity and the buoyancy, where ρ and ρ_P are the density of the air and the particles, respectively, and $\vec{F}_a$ stands for additional forces (per unit mass) that may be important. 6) where ζ is a Gaussian random number, and k is the turbulent kinetic energy. 7) where C_j is the mean particle concentration in a cell, V_j is the volume of a computational cell for particles, dt is the particle residence time, and subscript (i,j) represents the ith trajectory and the jth cell.

Research has shown that the two models yield essentially consistent calculation results at steady state,[84] but the Eulerian model requires shorter computation time. The Lagrangian model was found to be computationally slow due to the need to track the trajectories of numerous particles (typically twice as many as the number of grid points). Therefore, researchers have suggested that the Eulerian model is more suitable for use in steady-state conditions. However, for simulating the long-term unsteady diffusion of particles during coughing, the Lagrangian method exhibits higher computational efficiency.[84,85]

Table 10 summarizes the CFD simulation studies on the distribution of pollutants in commercial airliner cabins that have been published within recent decades. This literature

Table 10: Summary of CFD calculation of pollutant concentration in airliner cabins in literature retrieval.

Serial number	Research unit	Year	Cabin environment	Turbulence model	Calculation method for particle concentration	Particle size	Experimental verification	Wall subsidence
1	Purdue University[84]	2007	Double-aisle airliner	Standard k-ε	Lagrangian method, Eulerian method	1 μm	×	×
2	Purdue University[2]	2009	Double-aisle airliner	RNG k-ε	Lagrangian method	0.7 μm	√	×
3	Hong Kong University of Science and Technology[67]	2009	Double-aisle airliner	RNG k-ε	Lagrangian method	2, 6, 12, 28, 45, 87.5, 137.5, 225 μm	√	√
4	Purdue University[89]	2011	Double-aisle airliner	DES realizable k-ε	Lagrangian method	0.1, 0.7, 2.5, 5, 10, 20, 100 μm	√	√
5	Purdue University[90]	2011	Double-aisle airliner	RNG k-ε	Lagrangian method	0.4, 8, 30 μm	×	×
6	Villanova University[91]	2012	Double-aisle airliner	Standard k-ε	Lagrangian method	3, 10 μm	√	√
7	Purdue University[92]	2013	Single-aisle airliner	RNG k-ε, DES realizable k-ε, DES+	Lagrangian method, RNG+ Eulerian method	3 μm	√	×
8	Tsinghua University[93]	2014	Single-aisle airliner	RNG k-ε	Lagrangian method	1.5, 3, 6, 10, 14, 18, 22.5, 31.25, 43.75, 56 μm	×	√
9	Royal Melbourne Institute of Technology[94]	2017	Single-aisle airliner	RNG k-ε	Lagrangian method	3.5 μm	×	√
10	Purdue University[95]	2017	Single-aisle airliner Double-aisle airliner	Combination of standard k-ω model and RNG k-ε model	Eulerian method	——	×	×
11	Tianjin University[78]	2022	Single-aisle airliner	Realizable k-ε model	Eulerian method	1, 5 μm	√	√
11	Tianjin University[96]	2023	Single-aisle airliner Double-aisle airliner	RNG k-ε model	Lagrangian method	——	√	×

summary reveals that the application of Lagrangian and Eulerian methods to simulate particle transport has become a widely popular approach in recent years. Numerous scholars, both domestically and internationally, have conducted simulation studies on particle transport inside single- and double-aisle airliner cabins. These studies encompass particulate matter of various sizes ranging from 0.1 μm to 225 μm. The simulations have explored the spread of particulate matter of different sizes within the cabin, generated by activities such as passenger coughing, breathing, and movements of crew members.

3.3 Factors influencing the accuracy of simulation results

Generally, most researchers have attributed the significant discrepancy between simulation results and experimental results to experimental measurement errors, such as rough measurements of boundary conditions,[19,78] neglecting air leakage in airliner cabins, [78] and omitting crucial elements during the simplification of the simulation model.[78] The instability of boundary conditions has always been regarded as the primary cause of the discrepancy. Liu *et al*. calibrated the boundary conditions to fulfill the "three stabilities" criterion:[19] wall temperature stability, as illustrated in Fig. 5; stability of the air supply boundary, as depicted in Fig. 6; and a simple structure and uniform temperature of the dummy, as demonstrated in Fig. 7. The high-precision data obtained from airliner cabins have been widely utilized by researchers, leading to a near doubling of the accuracy of simulation results. For a comparison of simulation and experimental accuracy, please refer to Figs. 8 and 9. Table 11 presents the accuracy of simulation results after stabilization of the boundary conditions, which is nearly double the accuracy of the results with the relatively unstable boundary conditions.[46]

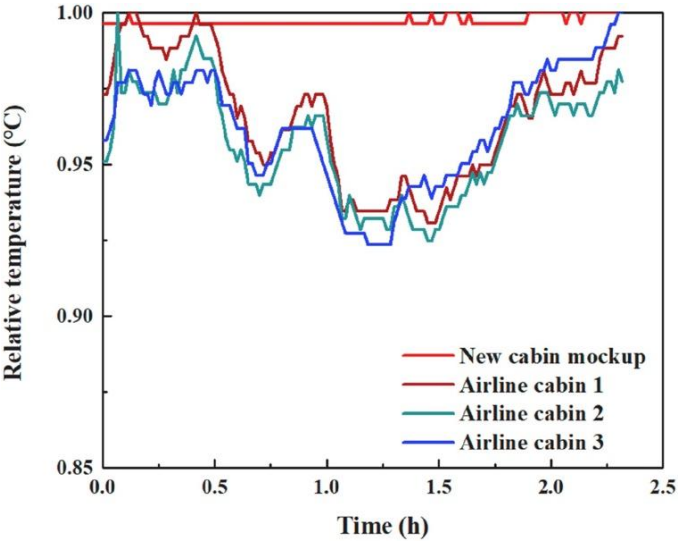

Fig. 5: Wall relative temperature as a function of time in the cabin mockup and other airliner cabins. Airliner cabin 1, airliner cabin 2 and airliner cabin 3 were three real airliner cabins.[19]

4. Comparison of various ventilation systems in airliner cabins

Currently, mixing ventilation is the most prevalent in airliner cabins. However, it has its drawbacks, including a strong draft sensation, low heat dissipation efficiency, and difficulty in discharging pollutants. Consequently, researchers have shifted their focus to other ventilation systems.

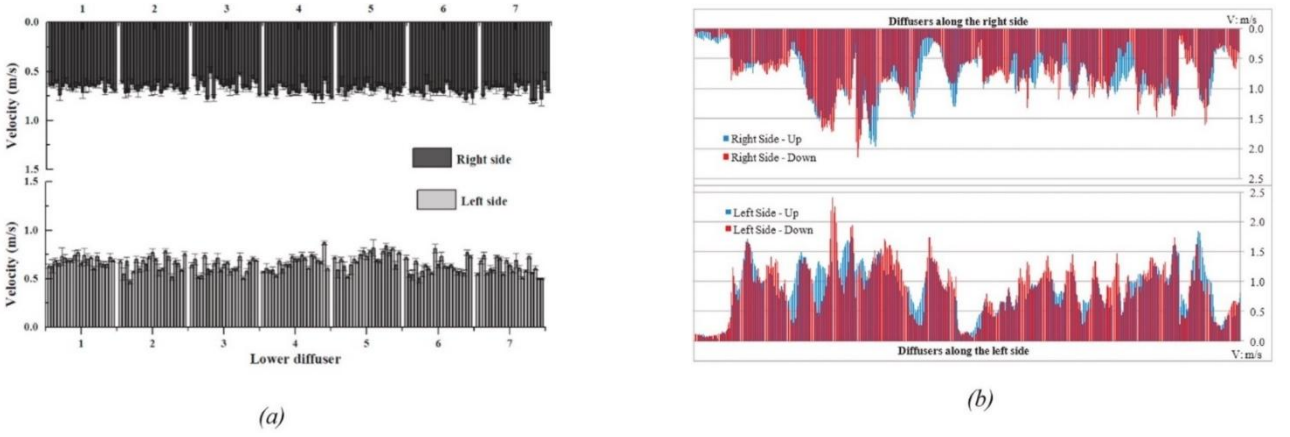

Fig. 6: Velocity distribution of supply air in the cabin mockup: (a) new cabin mockup; (b) other cabin mockups.[19,21]

Table 11: Error analysis between simulated and experimental values at the measurement points under different ventilation systems.[46]

Ventilation system	Absolute deviation of velocity (m/s)	Relative deviation of velocity (%)	Absolute deviation of temperature (°C)	Relative deviation of temperature (%)
CSMV	0.008	5.644	0.82	3.280
DV	0.021	67.524	0.59	2.116
MD-82-MV[23]	0.052	113.300	0.90	3.820

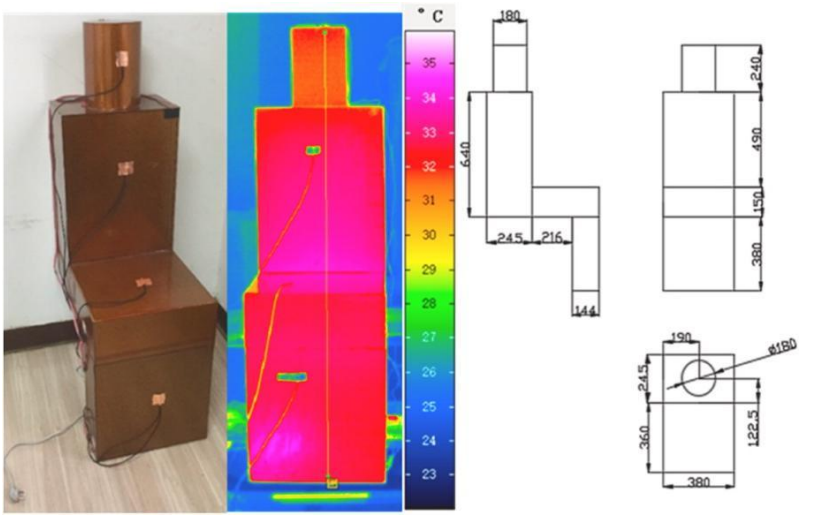

Fig. 7: Dummy at a constant temperature in the cabin mockup.[19]

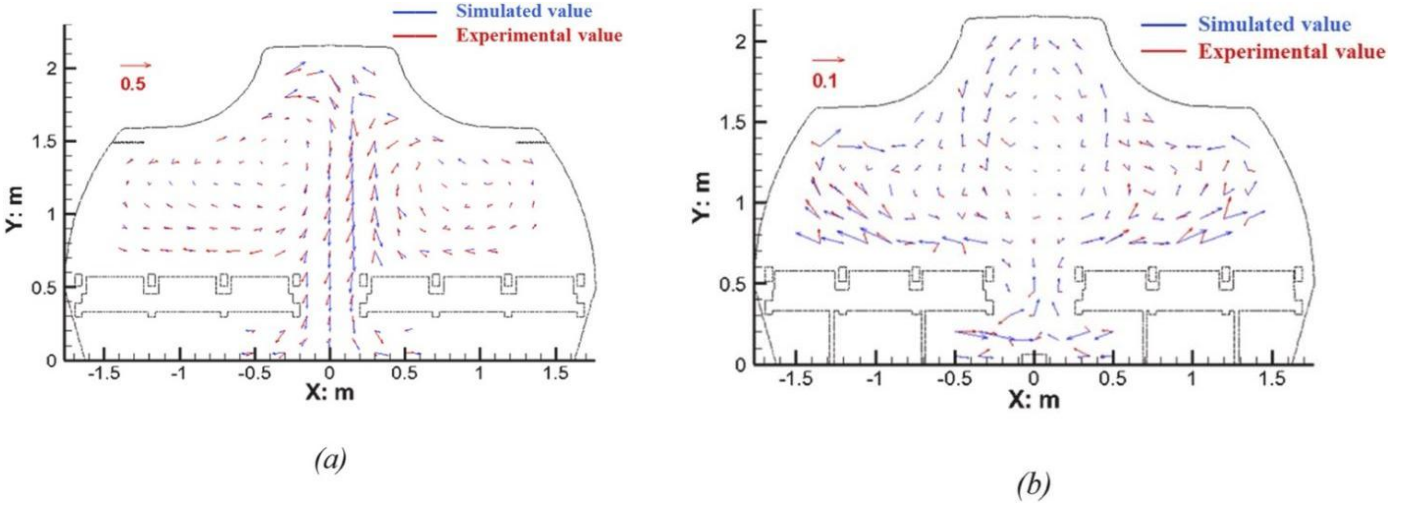

Fig. 8: Comparison of experimental and simulated values in the form of velocity vectors: (a) mixing ventilation and (b) displacement ventilation.[46]

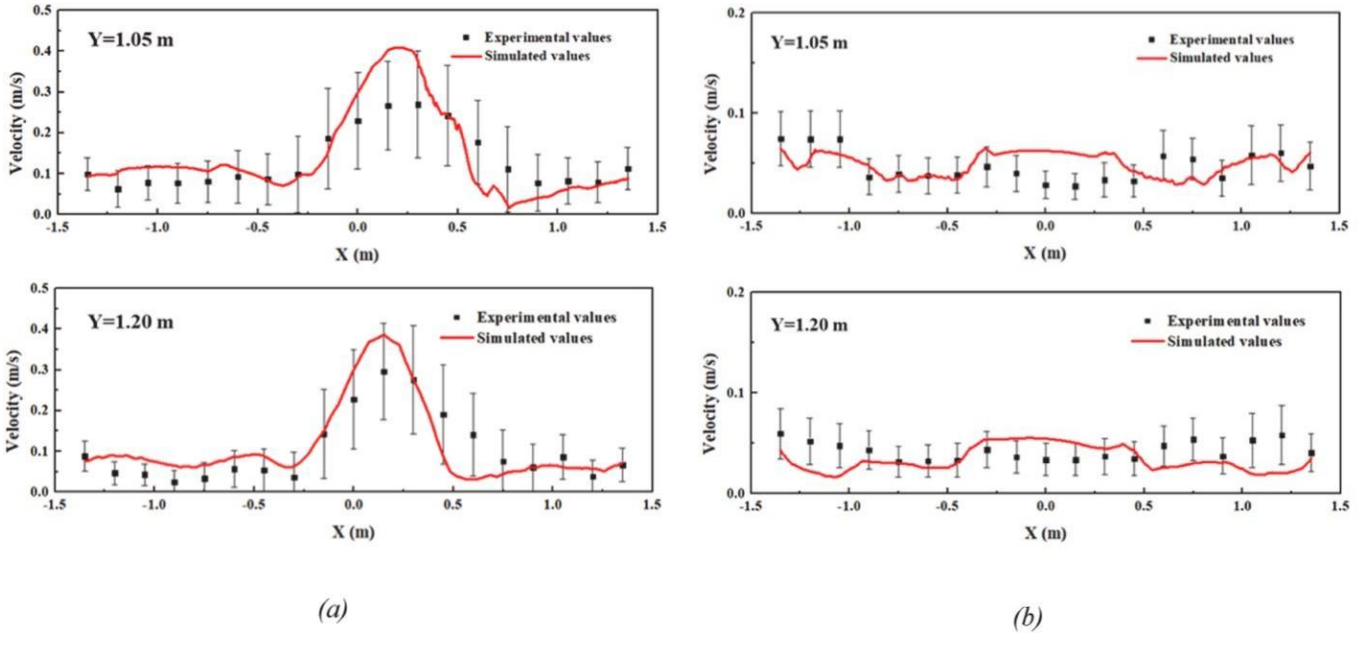

Fig. 9: Comparison of experimental and simulated velocity values: (a) mixing ventilation and (b) displacement ventilation.[46]

4.1 Evaluation indicators

Various evaluation indicators have been employed to compare different ventilation systems. These indicators encompass the assessment of air distribution, thermal comfort, and the evaluation of pollutant transmission and infection risk, as detailed in Table 12.

4.2 Comparison of different ventilation systems

To date, comprehensive research has been conducted on commonly used mixing ventilation systems, various displacement ventilation systems, personalized-ventilation systems, and other personalized air supply systems (such as the personal chair-armrest-embedded air system), as detailed

Table 12: Evaluation indicators.

Evaluation system	Evaluation parameters	Parameter definition	Calculation method
Airflow evaluation	Velocity nonuniformity index (VUI)[46,97]	Quantitatively analyze the distribution characteristics of the air velocity	$\bar{v}=\frac{\sum v_i}{n}$ $\delta_v=\sqrt{\frac{\sum(\bar{v}-v_i)^2}{n}}$ $VUI=\frac{\delta_v}{\bar{v}}$
	Temperature nonuniformity index (TUI)[46,97]	Quantitatively analyze the distribution characteristics of the temperatures	$\bar{T}=\frac{\sum T_i}{n}$ $\delta T=\sqrt{\frac{\sum(\bar{T}-T_i)^2}{n}}$ $TUI=\frac{\delta T}{\bar{T}}$
	Heat removal efficiency (HRE)[46,97]	Energy utilization of a ventilation system; temperature distribution uniformity and performance in discharging contaminants.	$\eta=\frac{T_e-T_s}{\bar{T}_i-T_s}$
	Mean air age[46,97]	Residence time of air	$\tau_i=\frac{\int_0^\infty c_i(t)dt}{c_i(0)}$
Thermal comfort evaluation	Draft rate (DR)[46,98-100]	Discomfort caused by the velocity of the airflow.	$DR=(34-T_a)\cdot(\bar{v}-0.05)^{0.62}\cdot(0.37\cdot\bar{v}\cdot Tu+3.14)$
	Percentage dissatisfied (PD)[45]	Function of the vertical air temperature difference between the head and ankles.	$PD=\frac{100}{1+exp(5.76-0.856\cdot\Delta T_{a,v})}$
Health evaluation	Risk assessment[46,99,101]	Infection risk for passengers in airliner cabins	$P=1-e^{(-C_i pt)}$

Note: 1) where n is the number of measurement points (-), v_i is the time-averaged velocity at each point (m/s), and $\bar{v}$ is the area-averaged velocity for all measurement points (m/s). 2) where T_i is the time-averaged temperature at each point (°C), and $\bar{T}$ is the area-averaged temperature for all measurement points (°C). 3) where T_e is the exhaust temperature (°C), T_s is the supply air temperature (°C), and $\bar{T}_i$ is the area-averaged temperature (°C). 4) where τ_i is the mean age of air (s), $c_i(t)$ is the SF_6 concentration at the measurement point (ppm), and $c_i(0)$ is the steady-state concentration at the beginning of the measurement (ppm). 5) where T_a is the local air temperature (°C), Tu is the local turbulence intensity (%), and $\Delta T_{a,v}$ is the vertical air temperature difference between head and ankles (°C). 6) where P is the infection risk for a passenger in an airliner cabin (-), C_i is the contaminant concentration (quantahour /m^3), p is the passenger's breathing flow rate (m^3/s), and t is the flight duration (s).

in Table 13. Gaspers are the small, circular, and adjustable vents above the passengers, which can provided personalized ventilation for each passenger,[95,102] as shown in Fig. 10. Researchers had discovered that while gaspers provide clean air, it may potentially pose negative impacts on passengers' health.[95,102,103] Meanwhile, the research had shown that the overall impact of opening gaspers on the average infection risk for passengers in personalized mixing ventilation systems is neutral.[95] In addition, relevant studies had confirmed that, to some extent, the implementation of gaspers can reduce the exposure risk of passengers in personalized displacement ventilation systems.[102,103]

Table 13: Characteristics of different ventilation systems.

Ventilation system	Schematic diagram	Characteristics
Sidewall supply and bottom return mixing ventilation (SMV)[45,97]	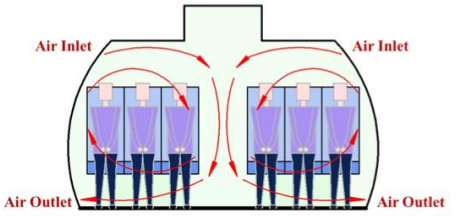	1)Strong draft sensation; 2)Low efficiency in pollutant removal; 3)Low level of dissatisfaction with thermal comfort.
Ceiling supply and bottom return mixing ventilation (CMV)[97]	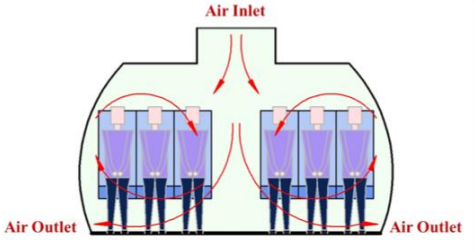	1)The air velocity in the aisle was high, while the air velocity around the passengers was low, resulting in insufficient fresh air reaching the passengers' surroundings; 2)There was a notable accumulation of heat; 3)The air age was relatively high, indicating poor ventilation efficiency.
Ceiling and sidewall supply and bottom return mixing ventilation (CSMV)[97]	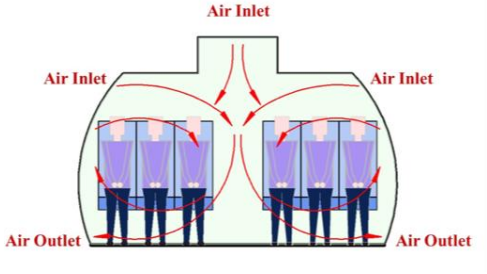	1)The air age was relatively low, indicating high ventilation efficiency; 2)There was less blowing sensation.
Displacement ventilation (DV)[45,97,104]	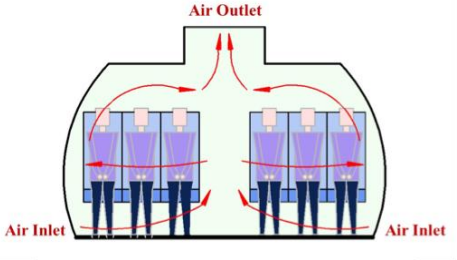	1)The overall velocity was significantly lower than that of mixing ventilation; 2)The air age was relatively low, indicating high ventilation efficiency; 3)High energy utilization efficiency; 4)Temperature stratification existed; 5)High heat removal efficiency and energy utilization efficiency; 6)High dissatisfaction with thermal comfort; 7)The disease infection was much lower than that under mixing ventilation.
Personalized displacement ventilation (proposed system: 2)[45]	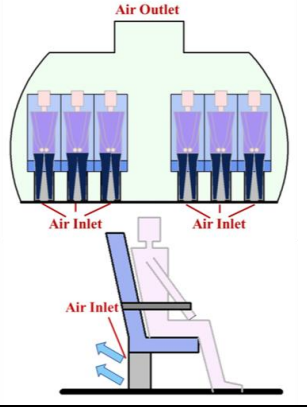	1)Passengers' legs felt cold; 2)Low flow rate; 3)Low probability of infectious disease transmission; 4)High pollutant removal efficiency; 5)Thermal comfort dissatisfaction fell between that of mixing ventilation and displacement ventilation.

Ventilation system	Schematic diagram	Characteristics
Personalized displacement ventilation (proposed system: 4)[45]	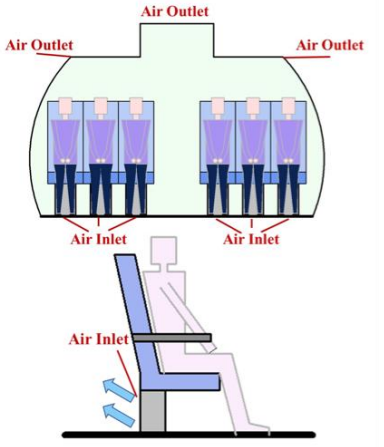	1)Passengers' legs felt cold; 2)Low flow rate; 3)Compared to the proposed system: 2, the probability of infectious disease transmission was lower; 4)High pollutant removal efficiency; 5)Thermal comfort dissatisfaction level fell between that of mixing ventilation and displacement ventilation.
Personalized displacement ventilation (proposed system: 6)[45]	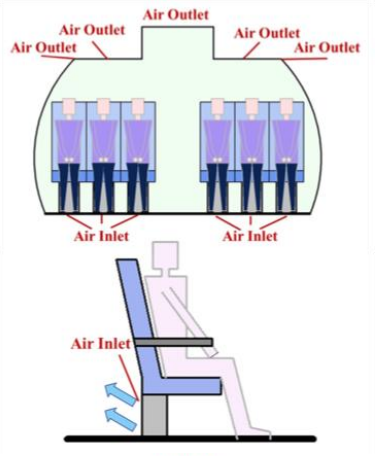	1)Passengers' legs felt cold; 2)Low flow rate; 3)The increase in exhaust outlets reduced the transmission probability of infectious diseases; 4)High pollutant removal efficiency; 5)Thermal comfort dissatisfaction fell between that of mixing ventilation and displacement ventilation.
Combination of MV and DV (MDV)[97,105]	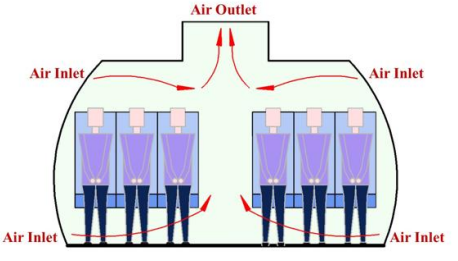	1)The air age was relatively low, indicating high ventilation efficiency; 2)Low flow rate; 3)High heat removal efficiency and energy utilization efficiency; 4)High dissatisfaction with thermal comfort; 5)Improved temperature stratification.
Personal chair-armrest-embedded air system[20]	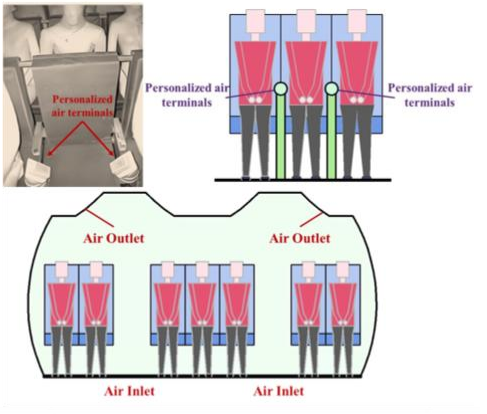	1)Temperature stratification existed; 2)Effective control of pollutants within the passengers' breathing zone, thereby reducing cross-infection.
Mixing and under-floor displacement air distribution systems[106]	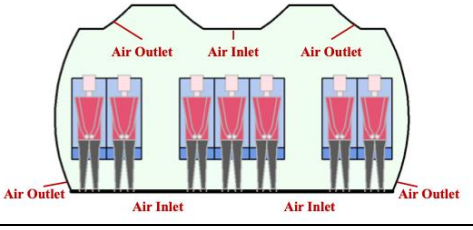	1)Low flow rate; 2)Less blowing sensation; 3)Temperature stratification existed.

Ventilation system	Schematic diagram	Characteristics
Personalized air distribution system[106]	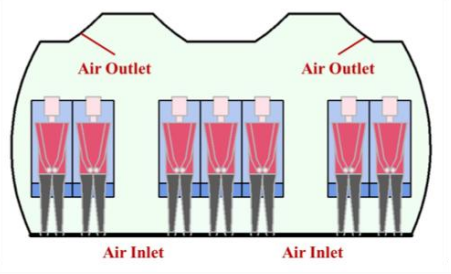	1)Low flow rate; 2)Less blowing sensation; 3)Temperature stratification existed. 4)It may be feasible to eliminate the spread of infectious diseases within the aircraft cabin.
Personalized mixing air distribution systems[107]	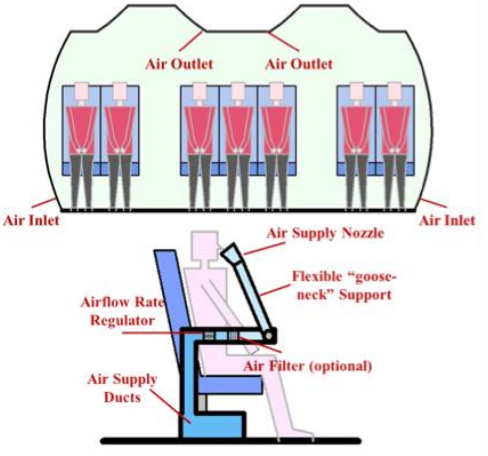	1)Low-velocity air supply nozzle is integrated with the seat; 2)Potentially reducing the infection probability.
Personalized and humidified air supply system [108]	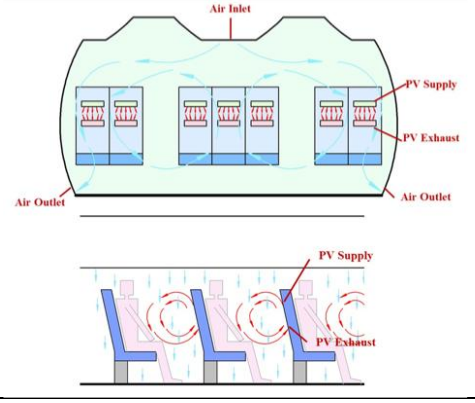	1)With a humidification function; 2)Potentially reducing the infection probability.

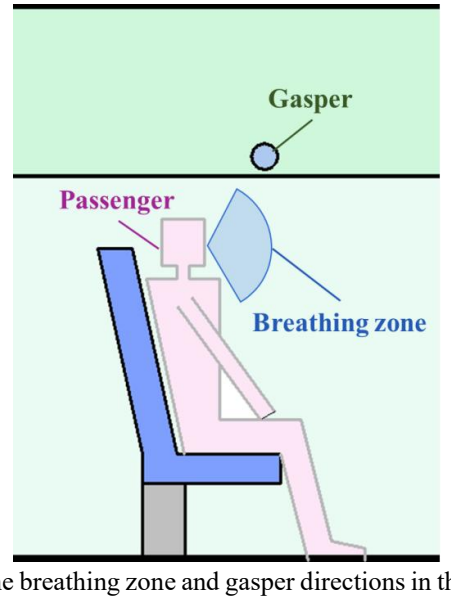

Fig. 10: The breathing zone and gasper directions in the side view.

5. Concept for a new airliner cabin air distribution system

Typically, the ECS in currently operational aircraft features a recirculation rate of 50% (*i.e.*, a blend of 50% outside air and 50% filtered inside air).[10] The current air distribution systems of ECS in airliner cabins employ a blend of fresh and return air to introduce temperature-regulated air into the cabin, ensuring a comfortable environment for both passengers and crew members. At the same time, the system's high air volume design has been found to enhance passengers' perception of drafts [109] and widen the spread of pollutants.[110] Additionally, the cabin's relative humidity remains excessively low,[10,111,112] compromising the comfort and well-being of passengers and crew. Despite improvements, there are still challenges in the use of enhanced air supply system, including difficulty in expelling pollutants,[113] pronounced drafts,[114] passenger discomfort,[19,114] and the risk of cross-infection from disease-carrying aerosols.[46]

During the design of traditional building air conditioning systems (all-air air conditioning system), a radiation air conditioning system with independent fresh air was proposed.[46] The radiant air distribution system has been widely applied in both residential and non-residential buildings, including offices, schools, and even large-scale structures like airports, train stations, and entrance halls.[115,116] In building air conditioning design, radiant surfaces are typically positioned on the floor or ceiling. Compared to traditional air conditioning systems, this system is capable of low-temperature heating and high-temperature cooling,[117] offering energy-saving potential.[118] Furthermore, when integrated with architectural design, this system simultaneously provides high thermal comfort and low system noise.[115,118,119] In addition, due to the low air supply flow rate, the radiation system can provide an ideal vertical air temperature gradient and mitigate the cold draft caused by excessive air flow,[120-122] as shown in Fig. 11. A survey conducted among users in adjacent buildings equipped with variable air volume (VAV) and radiant cooling systems revealed that the proportion of respondents in the "satisfied or very satisfied" category rose from 45% in areas with all-air systems to 63% in areas with radiant systems,[123] as illustrated in Fig. 12.

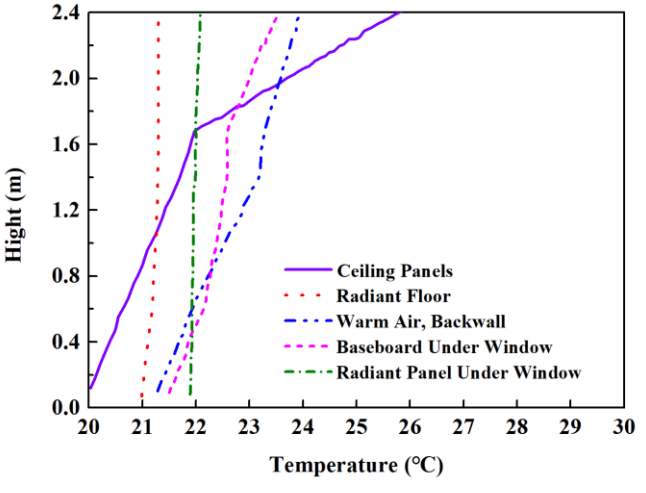

Fig. 11: Vertical air temperature differences measured in a test space for different heating systems (Data sourced from reference).[120]

This radiant system achieved the control of indoor parameters at constant values, including constant temperature, humidity, oxygen concentration, and cleanliness, through temperature regulation of cold and hot walls and the supply of fresh air. Studies confirmed that, under both radiation and fresh-air modes, the maximum temperature difference inside the room did not exceed 2.1 °C under cooling conditions, and did not exceed 3 °C under heating conditions.[46] The air conditioning system met the cooling and heating load requirements of the room. Additionally, its air distribution system exclusively comprised fresh air in the overall airflow, maintaining a low velocity throughout the premises, thereby ensuring a high degree of thermal comfort and consistent indoor temperature. Furthermore, this type of air distribution systems can be used in commercial airliner cabins. A conceptual diagram of the system's structure is displayed in Fig. 13.

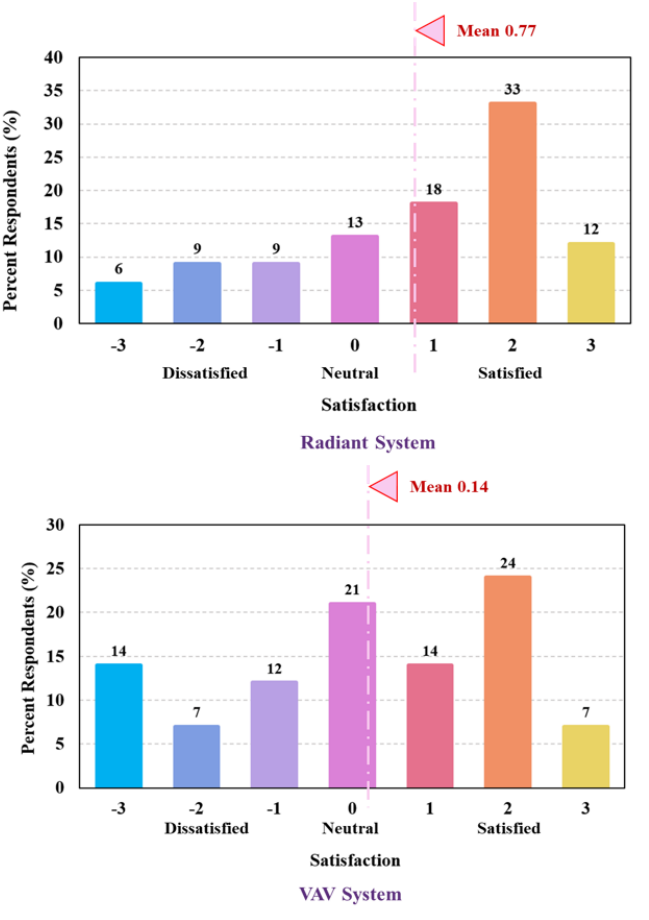

Fig. 12: Occupant survey results: comparison between VAV and Radiant system (Data sourced from reference).[123]

The proposed system resembles a fully fresh air system. The cabin is surrounded by cooling/heating medium pipes which provide cooling or heating through radiation. Only fresh air with adequate oxygen content is introduced into the cabin, resulting in a significantly lower air velocity compared to traditional air distribution systems in airliner cabins. Consequently, there is essentially no draft sensation. The cabin's heating or cooling system relies on radiant heating or cooling to achieve the desired cabin environment. The buried pipes can be located around the airliner cabin walls.

However, it is worth noting that in this radiation system, the medium for the refrigerant system must be carefully selected to prevent condensation and icing. Careful consideration should be given to the pipeline layout, including the diameter of the pipelines, the spacing between pipelines, and whether to arrange the pipelines in several modules. Moreover, since the system is a refrigerant one, particular emphasis must be placed on the overall weight of the system

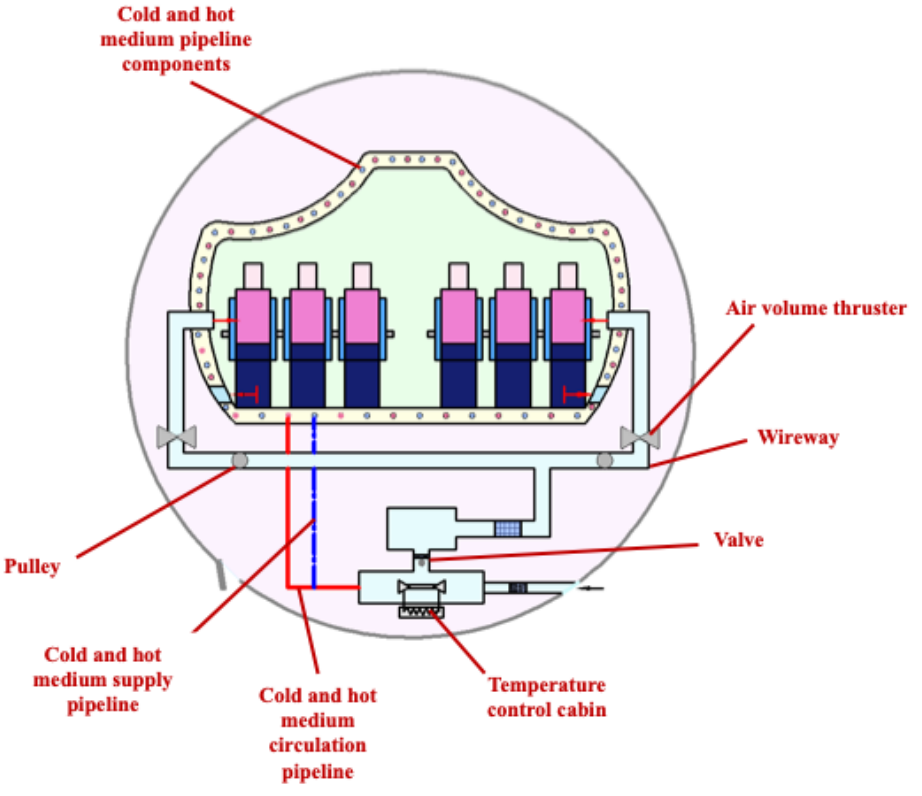

Fig. 13: Radiation air distribution system with independent fresh air for use in airliner cabins.

during aircraft design, along with considerations for issues like variations in refrigerant density resulting from pressure changes during high-altitude flights. Furthermore, the temperature of the cooling medium in the air distribution system should be designed to ensure the comfort of passengers in the airliner cabins. However, at the present stage, there are no relevant standard guidelines for this specific air distribution mode, especially for air distribution systems in airliner cabins. Additionally, the locations of the fresh air intake and exhaust outlets must be carefully designed to minimize the cross-transmission of pollutants. However, the official implementation of such a system still necessitates extensive research and development over an extended period, and it is presently only at the stage of being a conceptual proposal.

6. Conclusion

This study conducted a literature review that used existing knowledge to demonstrate the current status of research on air distribution systems in airliner cabins. Additionally, it presented the pros and cons of various air distribution systems according to the relevant investigations. This information will aid researchers in selecting the most appropriate systems for different scenarios. Papers selected for review were chosen subjectively from the scientific articles contained in the ScienceDirect and Web of Science databases. Learning about advancements in air distribution systems for airliner cabins will be beneficial for many young and experienced scientists, as has been the case with other reviews [111,124,125]. These reviews have served as an initial step for composing articles or conducting further research, while also highlighting the current shortcomings of air distribution systems in airliner cabins. Although the present review has not taken a definitive stance, it has explored several important areas: understanding the cabin environment and its associated standards, studying air distribution systems, evaluating different systems through existing research, and proposing novel concepts for air distribution systems in airliner cabins. This literature review has reinforced the following points:

The control requirements for air quality and ventilation systems are among the most pressing concerns today in airliner cabins, particularly the issue of relative humidity within the cabin, which deserves attention.

This paper demonstrated the primary research methodologies currently for air distribution systems in airliners in use. Furthermore, the review confirmed that increasing the precision of boundary conditions can indeed enhance simulation accuracy. This may represent a new trend in the design of cabins for simulation experiments in the future.

There are numerous options for improving the air distribution systems in cabins, and researchers can select different systems based on their needs.

The radiation air distribution system with independent fresh air for airliner cabins offers control of indoor parameters at constant values, potentially representing the future trend of the system in airliner cabins.

By further organizing relevant scientific findings, this study aimed to facilitate the advancement of future research on improvements to airliner cabin environments. This paper posits that advancements in cabin air distribution systems are

effective ways to enhance travel environments, improve thermal comfort, and reduce the risk of cross-infection with infectious diseases.

Acknowledgements
This study was supported by the Talent Introduction Project of Changzhou University through Grant No. ZMF23020068. This study was also supported by the China Postdoctoral Science Foundation through Grant No. 2024M750437.

Conflict of Interest
There is no conflict of interest.

Supporting Information
Applicable.

CRediT Statement
Mingxin Liu: Data curation, Data visualization, Formal analysis, Methodology, Funding acquisition, Writing – original draft. **Xingwang Zhao:** Resources, Funding acquisition, Writing – review & editing. **Yongzhi Zhang:** Data curation, Validation, Writing – review, Supervision. & editing.

References
[1] F. Zhang, D. J. Graham, Air transport and economic growth: a review of the impact mechanism and causal relationships, *Transport Reviews*, 2020, **40**, 506-528, doi: 10.1080/01441647.2020.1738587.
[2] Z. Zhang, X. Chen, S. Mazumdar, T. Zhang, Q. Chen, Experimental and numerical investigation of airflow and contaminant transport in an airliner cabin mockup, *Building and Environment*, 2009, **44**, 85-94, doi: 10.1016/j.buildenv.2008.01.012.
[3] S. L. Mcfarland. Airliner cabin air quality exposure assessment, The University of Texas School of Public Health, Houston, USA, 2005.
[4] N. Yu, Y. Zhang, M. Zhang, H. Li, Thermal condition and air quality investigation in commercial airliner cabins, *Sustainability*, 2021, **13**, 7047, doi: 10.3390/su13137047.
[5] H. Wang, J. Wang, Z. Feng, F. Haghighat, S. Cao, Intelligent anti-infection ventilation strategy based on computer audition: Towards healthy built environment and low carbon emission, *Sustainable Cities and Society*, 2023, **99**, 104888, doi: 10.1016/j.scs.2023.104888.
[6] F. Wang, F. Chen, T. Zhang, An aisle displacement ventilation system for twin-aisle commercial airliner cabin, *Building and Environment*, 2022, **223**, 109439, doi: 10.1016/j.buildenv.2022.109439.
[7] X. Zhang, J. Liu, X. Liu, C. Liu, Q. Chen, HEPA filters for airliner cabins: State of the art and future development, *Indoor Air*, 2022, **32**, e13103, doi: 10.1111/ina.13103.
[8] A.S.S.P. Committee, ANSI/ASHRAE Standard 161-2023 Air Quality within Commercial Aircraft, New York, USA, ASHRAE Standing Standard Project Committee, 2023.
[9] A.T. Committees, 2019 ASHRAE HANDBOOK Heating, Ventilating, and Air-Conditioning APPLICATIONS, ASHRAE Atlanta, USA, 2019.
[10] M. Liu, J. Liu, J. Ren, L. Liu, R. Chen, Y. Li, Bacterial community in commercial airliner cabins in China, *International Journal of Environmental Health Research*, 2020, **30**, 284-295, doi: 10.1080/09603123.2019.1593329.
[11] P. Wolkoff, S. K. Kjærgaard, The dichotomy of relative humidity on indoor air quality, *Environment International*, 2007, **33**, 850-857, doi: 10.1016/j.envint.2007.04.004.
[12] T. Lindgren, D. Norback, Health and perception of cabin air quality among Swedish commercial airline crew, *Indoor Air*, 2005, **15**, 65-72, doi: 10.1111/j.1600-0668.2005.00353.x.
[13] E. A. Whelan, C. C. Lawson, B. Grajewski, M. R. Petersen, L. E. Pinkerton, E. M. Ward, T. M. Schnorr, Prevalence of respiratory symptoms among female flight attendants and teachers, *Occupational and Environmental Medicine*, 2003, **60**, 929-934, doi: 10.1136/oem.60.12.929.
[14] T. Lindgren, D. Norbäck, G. Wieslander, Perception of cabin air quality in airline crew related to air humidification, on intercontinental flights, *Indoor Air*, 2007, **17**, 204-210, doi: 10.1111/j.1600-0668.2006.00467.x.
[15] C.a.a.O. China, Chinese civil aviation regulations Part 25 airworthiness standards for transport aircraft, Beijing, China: Civil Aviation Administration of China, 2016.
[16] F.A. Administration, Federal Aviation Regulations (FAR) Part 25 Airworthiness standards: Transport category airplanes, Washington, USA: Federal Aviation Administration, 2024.
[17] T.a.a.D.I.a.O.E.S. (Asd-Stan), prEN 4618: Aerospace series - Aircraft internal air quality standards, criteria and determination methods, Brussels, Belgium: the Aerospace and Defence Industries Association of Europe - Standardization (ASD-STAN), 2013.
[18] E.U.A.S. Agency, CS-25 Certification Specifications and Acceptable Means of Compliance for Large Aeroplanes, Cologne, Germany: European Union Aviation Safety Agency, 2023.
[19] M. Liu, D. Chang, J. Liu, S. Ji, C. Lin, D. Wei, Z. Long, T. Zhang, X. Shen, Q. Cao, X. Li, X. Zeng, H. Li, Experimental investigation of air distribution in an airliner cabin mockup with displacement ventilation, *Building and Environment*, 2021, **191**, 107577, doi: 10.1016/j.buildenv.2020.107577.
[20] T. Zhang, P. Li, S. Wang, A personal air distribution system with air terminals embedded in chair armrests on commercial airplanes, *Building and Environment*, 2012, **47**, 89-99, doi: 10.1016/j.buildenv.2011.04.035.
[21] W. Liu, J. Wen, J. Chao, W. Yin, C. Shen, D. Lai, C.-H. Lin,

J. Liu, H. Sun, Q. Chen, Accurate and high-resolution boundary conditions and flow fields in the first-class cabin of an MD-82 commercial airliner, *Atmospheric Environment*, 2012, **56**, 33-44, doi: 10.1016/j.atmosenv.2012.03.039.

[22] R. P. Garner, K. L. Wong, S. C. Ericson, A. J. Baker, J. A. Orzechowski. CFD validation for contaminant transport in aircraft cabin ventilation flow fields, *Safe Association 41st Annual Symposium*, September 22-24, Jacksonville, Florida, USA, 2004, 1-6.

[23] W. Liu, J. Wen, C. Lin, J. Liu, Z. Long, Q. Chen, Evaluation of various categories of turbulence models for predicting air distribution in an airliner cabin, *Building and Environment*, 2013, **65**, 118-131, doi: 10.1016/j.buildenv.2013.03.018.

[24] C. Wang, J. Zhang, H. Chen, J. Liu, Experimental study of thermo-fluid boundary conditions, airflow and temperature distributions in a single aisle aircraft cabin mockup, *Indoor and Built Environment*, 2021, **30**, 1185-1199, doi: 10.1177/1420326x20932271.

[25] C. H. Lin, K. Dunn, R. Horstman, J. Topmiller, M. Ahlers, J. Bennett, L. Sedgwick, S. Wirogo, Numerical Simulation of Airflow and Airborne Pathogen Transport in Aircraft Cabins--Part I: Numerical Simulation of the Flow Field, *ASHRAE Transactions*, 2005, **111**, 755-763.

[26] R. H. G. Muller, T. Scherer, T. Rotger, O. Schaumann, M. Markwart, Large body aircraft cabin a/c flow measurement by helium bubble tracking, *Journal of Flow Visualization and Image Processing*, 1997, **4**, 295-306, doi: 10.1615/jflowvisimageproc.v4.i3.90.

[27] G. Günther, J. Bosbach, J. Pennecot, C. Wagner, T. Lerche, I. Gores, Experimental and numerical simulations of idealized aircraft cabin flows, *Aerospace Science and Technology*, 2006, **10**, 563-573, doi: 10.1016/j.ast.2006.02.003.

[28] J. Bosbach, J. Pennecot, C. Wagner, M. Raffel, T. Lerche, S. Repp, Experimental and numerical simulations of turbulent ventilation in aircraft cabins, *Energy*, 2006, **31**, 694-705, doi: 10.1016/j.energy.2005.04.015.

[29] G. N. Sze To, M. P. Wan, C. Y. H. Chao, L. Fang, A. Melikov, Experimental study of dispersion and deposition of expiratory aerosols in aircraft cabins and impact on infectious disease transmission, *Aerosol Science and Technology*, 2009, **43**, 466-485, doi: 10.1080/02786820902736658.

[30] C. H. Lin, T. T. Wu, R. H. Horstman, P. A. Lebbin, M. H. Hosni, B. W. Jones, B. T. Beck, Comparison of large eddy simulation predictions with particle image velocimetry data for the airflow in a generic cabin model, *HVAC&R Research*, 2006, **12**, 935-951, doi: 10.1080/10789669.2006.10391218.

[31] Y. M. Gbamele´, P. Desevaux, J.-P. Prenel, A method for validating two-dimensional flow configurations in particle streak velocimetry, *Journal of Fluids Engineering*, 2000, **122**, 438-439, doi: 10.1115/1.483279.

[32] E. R. Ramer, F. D. Shaffer, Automated analysis of multiple-pulse particle image velocimetry data, *Applied Optics*, 1992, **31**, 779-784.

[33] J. Li, J. Liu, C. Wang, N. Jiang, X. Cao, PIV methods for quantifying human thermal plumes in a cabin environment without ventilation, *Journal of Visualization*, 2017, **20**, 535-548, doi: 10.1007/s12650-016-0404-4.

[34] X. Cao, J. Liu, J. Pei, Y. Zhang, J. Li, X. Zhu, 2D-PIV measurement of aircraft cabin air distribution with a high spatial resolution, *Building and Environment*, 2014, **82**, 9-19, doi: 10.1016/j.buildenv.2014.07.027.

[35] X. Cao, J. Li, J. Liu, W. Yang, 2D-PIV measurement of isothermal air jets from a multi-slot diffuser in aircraft cabin environment, *Building and Environment*, 2016, **99**, 44-58, doi: 10.1016/j.buildenv.2016.01.018.

[36] X. Cao, J. Liu, N. Jiang, Q. Chen, Particle image velocimetry measurement of indoor airflow field: a review of the technologies and applications, *Energy and Buildings*, 2014, **69**, 367-380, doi: 10.1016/j.enbuild.2013.11.012.

[37] J. Li, X. Cao, J. Liu, C. Wang, Y. Zhang, Global airflow field distribution in a cabin mock-up measured *via* large-scale 2D-PIV, *Building and Environment*, 2015, **93**, 234-244, doi: 10.1016/j.buildenv.2015.06.030.

[38] S. B. Poussou, S. Mazumdar, M. W. Plesniak, P. E. Sojka, Q. Chen, Flow and contaminant transport in an airliner cabin induced by a moving body: Model experiments and CFD predictions, *Atmospheric Environment*, 2010, **44**, 2830-2839, doi: 10.1016/j.atmosenv.2010.04.053.

[39] J. Li, J. Liu, C. Wang, M. Wesseling, D. Müller, PIV experimental study of the large-scale dynamic airflow structures in an aircraft cabin: Swing and oscillation, *Building and Environment*, 2017, **125**, 180-191, doi: 10.1016/j.buildenv.2017.07.043.

[40] A. Wang, Y. Zhang, Y. Sun, Streak Recognition for a three-dimensional volumetric particle tracking velocimetry system, *ASHRAE Transactions*, 2005, **111**, 476.

[41] J. Bosbach, M. Kühn, C. Wagner, Large scale particle image velocimetry with helium filled soap bubbles, *Experiments in Fluids*, 2009, **46**, 539-547, doi: 10.1007/s00348-008-0579-0.

[42] W. Coetzee, R. L. J. Coetzer, R. Rawatlal, Response surface strategies in constructing statistical bubble flow models for the development of a novel bubble column simulation approach, *Computers & Chemical Engineering*, 2012, **36**, 22-34, doi: 10.1016/j.compchemeng.2011.07.014.

[43] Y. Huang, X. Shen, J. Li, B. Li, R. Duan, C.-H. Lin, J. Liu, Q. Chen, A method to optimize sampling locations for measuring indoor air distributions, *Atmospheric Environment*, 2015, **102**, 355-365, doi: 10.1016/j.atmosenv.2014.12.017.

[44] X. Zhu, The Experimental Research about the Influence of Natural Convection on the Flow Field in the Cabin Mockup, Tianjin, China, Tianjin University, 2016.
[45] R. You, Y. Zhang, X. Zhao, C. H. Lin, D. Wei, J. Liu, Q. Chen, An innovative personalized displacement ventilation system for airliner cabins, *Building and Environment*, 2018, **137**, 41-50, doi: 10.1016/j.buildenv.2018.03.057.
[46] M. Liu, J. Liu, Q. Cao, X. Li, S. Liu, S. Ji, C. H. Lin, D. Wei, X. Shen, Z. Long, Q. Chen, Evaluation of different air distribution systems in a commercial airliner cabin in terms of comfort and COVID-19 infection risk, *Building and Environment*, 2022, **208**, 108590, doi: 10.1016/j.buildenv.2021.108590.
[47] W. Liu, Simulation and Inverse Design on Air Distribution in Commercial Airliner Cabins, Tianjin, China, Tianjin University, 2016.
[48] D. Chang, Experimental study on flow field under mixing/displacement ventilation, Tianjin, China, Tianjin University, 2019.
[49] Y. Chen, Construction and Experimental Study of a Commercial Aircraft Cabin Mockup, Tianjin, China, Tianjin University, 2012.
[50] C. Wang, Experimental and Numerical Study on Unsteady Airflow around Passengers in the Aircraft Cabin. Tianjin, China, Tianjin University, 2017.
[51] X. Li, T. Zhang, M. Fan, M. Liu, D. Chang, Z. Wei, C. H. Lin, S. Ji, J. Liu, S. Shen, Z. Long, Experimental evaluation of particle exposure at different seats in a single-aisle aircraft cabin, *Building and Environment*, 2021, **202**, 108049, doi: 10.1016/j.buildenv.2021.108049.
[52] Y. Zhang, J. Liu, J. Pei, C. Wang, Statistical analysis of turbulent thermal convection in a cabin mockup, *Building and Environment*, 2017, **115**, 34-41, doi: 10.1016/j.buildenv.2017.01.012.
[53] T. Mizine, M. Warfield, Development of three-dimensional thermal airflow analysis computer program and verification test, *ASHRAE Transactions*, 1992, **96**, 1-10.
[54] A. Singh, M. H. Hosni, R. H. Horstman, Numerical simulation of airflow in an aircraft cabin section/Discussion, *ASHRAE Transactions*, 2002, **108**, 1005-1013.
[55] H. Mo, M. Hosni, B. Jones, Application of particle image velocimetry for the measurement of the airflow characteristics in an aircraft cabin, *ASHRAE Transactions*, 2003, **109**, 101-110.
[56] A. Wang, Y. Zhang, Y. Sun, X. Wang, Experimental study of ventilation effectiveness and air velocity distribution in an aircraft cabin mockup, *Building and Environment*, 2008, **43**, 337-343, doi: 10.1016/j.buildenv.2006.02.024.
[57] S. Mazumdar, Q. Chen, Influence of cabin conditions on placement and response of contaminant detection sensors in a commercial aircraft, *Journal of Environmental Monitoring Jem,* 2008, **10**, 71-81, doi: 10.1039/b713187a.
[58] M. Kühn, J. Bosbach, C. Wagner, Experimental parametric study of forced and mixed convection in a passenger aircraft cabin mock-up, *Building and Environment*, 2009, **44**, 961-970, doi: 10.1016/j.buildenv.2008.06.020.
[59] M. Rosenstiel, R.-R. Grigat, Segmentation and classification of streaks in a large-scale particle streak tracking system, *Flow Measurement and Instrumentation*, 2010, **21**, 1-7, doi: 10.1016/j.flowmeasinst.2009.10.001.
[60] J. Bosbach, S. Lange, T. Dehne, G. Lauenroth, F. Hesselbach, M. Allzeit, Alternative ventilation concepts for aircraft cabins, *CEAS Aeronautical Journal*, 2013, **4**, 301-313, doi: 10.1007/s13272-013-0074-z.
[61] A. L. Koch, What size should a bacterium be? A question of scale, *Annual Review of Microbiology*, 1996, **50**, 317-348, doi: 10.1146/annurev.micro.50.1.317.
[62] W. Kowalski, W.P. Bahnfleth, T. Whittam, Filtration of airborne microorganisms: modeling and prediction, *Ashrae Trans*, 1999, **105**, 4-17.
[63] S. Murakami, D. Eng, S. Kato, Y. Tanaka, Diffusion characteristics of airborne particles with gravitational settling in a convection-dominant indoor flow field, *ASHRAE Transactions*, 1992, **98**, 1-16.
[64] R. W. Powell, B. W. Jones, M. H. Hosni, Measurement of particle deposition rates in a commercial aircraft cabin, *HVAC&R Research*, 2014, **20**, 770-779, doi: 10.1080/10789669.2014.945851.
[65] T. Chang, C. Tsai, C. Wu, L. Chang, K. Chuang, H. Chuang, L. Young, Development of land-use regression models to estimate particle mass and number concentrations in Taichung, Taiwan, *Atmospheric Environment*, 2021, **252**, 118303, doi: 10.1016/j.atmosenv.2021.118303.
[66] T. Glytsos, J. Ondráček, L. Džumbová, K. Eleftheriadis, M. Lazaridis, Fine and coarse particle mass concentrations and emission rates in the workplace of a detergent industry, *Indoor and Built Environment*, 2014, **23**, 881-889, doi: 10.1177/1420326x13483765.
[67] M. P. Wan, G. N. Sze To, C. Y. H. Chao, L. Fang, A. Melikov, Modeling the fate of expiratory aerosols and the associated infection risk in an aircraft cabin environment, *Aerosol Science and Technology*, 2009, **43**, 322-343, doi: 10.1080/02786820802641461.
[68] J. M. Beneke, B. W. Jones, M. Hosni, Fine particle dispersion in a commercial aircraft cabin, *HVAC&R Research*, 2011, **17**, 107-117, doi: 10.1080/10789669.2011.543255.
[69] F. Li, J. Liu, J. Pei, C. Lin, Q. Chen, Experimental study of gaseous and particulate contaminants distribution in an aircraft cabin, *Atmospheric Environment*, 2014, **85**, 223-233, doi: 10.1016/j.atmosenv.2013.11.049.

[70] Q. Chen, J. Srebric, A procedure for verification, validation, and reporting of indoor environment CFD analyses, *HVAC&R Research*, 2002, **8**, 201-216, doi: 10.1080/10789669.2002.10391437.

[71] A. C. K. Lai, W. W. Nazaroff, Supermicron particle deposition from turbulent chamber flow onto smooth and rough vertical surfaces, *Atmospheric Environment*, 2005, **39**, 4893-4900, doi: 10.1016/j.atmosenv.2005.04.036.

[72] M. Chen, Y. Shi, L. Dong, Q. Wang, Flash pyrolysis of Fushun oil shale fine particles in an experimental fluidized-bed reactor, *Oil Shale*, 2010, **27**, 297-308, doi: 10.3176/oil.2010.4.03.

[73] M. Tang, S. C. Chen, D. Y. H. Pui, An improved atomizer with high output of nanoparticles, *Journal of Aerosol Science*, 2018, **124**, 10-16, doi: 10.1016/j.jaerosci.2018.07.001.

[74] W. Liu, S. Mazumdar, Z. Zhang, S. B. Poussou, J. Liu, C.-H. Lin, Q. Chen, State-of-the-art methods for studying air distributions in commercial airliner cabins, *Building and Environment*, 2012, **47**, 5-12, doi: 10.1016/j.buildenv.2011.07.005.

[75] C. Wu, N. A. Ahmed, Numerical study of transient aircraft cabin flowfield with unsteady air supply, *Journal of Aircraft*, 2011, **48**, 1994-2001, doi: 10.2514/1.C031415.

[76] K. Ebrahimi, Z. C. Zheng, M. H. Hosni, A computational study of turbulent airflow and tracer gas diffusion in a generic aircraft cabin model, *Journal of Fluids Engineering*, 2013, **135**, 111105, doi: 10.1115/1.4025096.

[77] Z. Shi, J. Chen, Q. Chen, On the turbulence models and turbulent Schmidt number in simulating stratified flows, *Journal of Building Performance Simulation*, 2016, **9**, 134-148, doi: 10.1080/19401493.2015.1004109.

[78] Q. Cao, M. Liu, X. Li, C. Lin, D. Wei, S. Ji, T. Zhang, Q. Chen, Influencing factors in the simulation of airflow and particle transportation in aircraft cabins by CFD, *Building and Environment*, 2022, **207**, 108413, doi: 10.1016/j.buildenv.2021.108413.

[79] J. Li, J. Liu, J. Pei, K. Mohanarangam, W. Yang, Experimental study of human thermal plumes in a small space *via* large-scale TR PIV system, *International Journal of Heat and Mass Transfer*, 2018, **127**, 970-980, doi: 10.1016/j.ijheatmasstransfer.2018.07.138.

[80] P. A. Durbin, B. P. Reif, Statistical theory and modeling for turbulent flows, John Wiley & Sons, 2011, ISBN: 1119957524.

[81] C. Wang, J. Liu, J. Li, Y. Guo, N. Jiang, Turbulence characterization of instantaneous airflow in an aisle of an aircraft cabin mockup, *Building and Environment*, 2017, **116**, 207-217, doi: 10.1016/j.buildenv.2017.02.015.

[82] M. Liu, J. Li, J. Liu, M. A. Hassan, Turbulence characterization of instantaneous airflow above passengers with different air distribution systems in a commercial airliner cabin, *Physics of Fluids*, 2023, **35**, 085118, doi: 10.1063/5.0159621.

[83] A. J. Deninger, S. Månsson, J. S. Petersson, G. Pettersson, P. Magnusson, J. Svensson, B. Fridlund, G. Hansson, I. Erjefeldt, P. Wollmer, K. Golman, Quantitative measurement of regional lung ventilation using 3He MRI, *Magnetic Resonance in Medicine: An Official Journal of the International Society for Magnetic Resonance in Medicine*, 2002, **48**, 223-232.doi.org/10.1002/mrm.10206.

[84] Z. Zhang, Q. Chen, Comparison of the Eulerian and Lagrangian methods for predicting particle transport in enclosed spaces, *Atmospheric Environment*, 2007, **41**, 5236-5248, doi: 10.1016/j.atmosenv.2006.05.086.

[85] M. Wang, C.-H. Lin, Q. Chen, Advanced turbulence models for predicting particle transport in enclosed environments, *Building and Environment*, 2012, **47**, 40-49, doi: 10.1016/j.buildenv.2011.05.018.

[86] T. Chan-Mou, Mean value and correlation problems connected with the motion of small particles suspended in a turbulent fluid, Delft, 1947, ISBN: 9789401757379.

[87] J. Hinze, M. S. Uberoi, Turbulence, *Journal of Applied Mechanics*, 1975, **27**, 256-275, doi:10.1115/1.3644063.

[88] A. C. K. Lai, W. W. Nazaroff, Modeling indoor particle deposition from turbulent flow onto smooth surfaces, *Journal of Aerosol Science*, 2000, **31**, 463-476, doi: 10.1016/S0021-8502(99)00536-4.

[89] M. Wang, C.-H. Lin, Q. Chen, Determination of particle deposition in enclosed spaces by Detached Eddy Simulation with the Lagrangian method, *Atmospheric Environment*, 2011, **45**, 5376-5384, doi: 10.1016/j.atmosenv.2011.06.042.

[90] J. K. Gupta, C. Lin, Q. Chen, Transport of expiratory droplets in an aircraft cabin, *Indoor Air*, 2011, **21**, 3-11, doi: 10.1111/j.1600-0668.2010.00676.x.

[91] K. Ebrahimi, Z. C. Zheng, M. H. Hosni, Computational Study of the Effects of Particle Size, Particle Injection Configuration, and Operating Pressure Gradient on Turbulent Dispersion of Spherical Micron-Sized Particles in a Generic Mockup Aircraft Cabin, *ASME International Mechanical Engineering Congress and Exposition, American Society of Mechanical Engineers*, Houston, Texas, USA, 2012, ISBN: 978-0-7918-4523-3.

[92] C. Chen, W. Liu, F. Li, C. Lin, J. Liu, J. Pei, Q. Chen, A hybrid model for investigating transient particle transport in enclosed environments, *Building and Environment*, 2013, **62**, 45-54, doi: 10.1016/j.buildenv.2012.12.020.

[93] Z. Han, G. N. To, S. C. Fu, C. Y. Chao, W. Weng, Q. Huang, Effect of human movement on airborne disease transmission in an airplane cabin: study using numerical modeling and quantitative risk analysis, *BMC Infectious Diseases*, 2014, **14**, 434, doi: 10.1186/1471-2334-14-434.

[94] Y. Yan, X. Li, Y. Shang, J. Tu, Evaluation of airborne disease infection risks in an airliner cabin using the Lagrangian-based Wells-Riley approach, *Building and Environment*, 2017, **121**, 79-92, doi: 10.1016/j.buildenv.2017.05.013.

[95] R. You, J. Chen, C. Lin, D. Wei, Q. Chen, Investigating the impact of gaspers on cabin air quality in commercial airliners with a hybrid turbulence model, *Building and Environment*, 2017, **111**, 110-122, doi: 10.1016/j.buildenv.2016.10.018.

[96] F. Wang, T. Zhang, R. You, Q. Chen, Evaluation of infection probability of Covid-19 in different types of airliner cabins, *Building and Environment*, 2023, **234**, 110159, doi: 10.1016/j.buildenv.2023.110159.

[97] Y. Zhang, J. Liu, J. Pei, J. Li, C. Wang, Performance evaluation of different air distribution systems in an aircraft cabin mockup, *Aerospace Science and Technology*, 2017, **70**, 359-366, doi: 10.1016/j.ast.2017.08.009.

[98] X. Kong, C. Guo, Z. Lin, S. Duan, J. He, Y. Ren, J. Ren, Experimental study on the control effect of different ventilation systems on fine particles in a simulated hospital ward, *Sustainable Cities and Society*, 2021, **73**, 103102, doi: 10.1016/j.scs.2021.103102.

[99] R. You, C. Lin, D. Wei, Q. Chen, Evaluating the commercial airliner cabin environment with different air distribution systems, *Indoor Air*, 2019, **29**, 840-853, doi: 10.1111/ina.12578.

[100] P. O. Fanger, A. K. Melikov, H. Hanzawa, J. Ring, Air turbulence and sensation of draught, *Energy and Buildings*, 1988, **12**, 21-39, doi: 10.1016/0378-7788(88)90053-9.

[101] T. Lim, J. Cho, B. S. Kim, The predictions of infection risk of indoor airborne transmission of diseases in high-rise hospitals: Tracer gas simulation, *Energy and Buildings*, 2010, **42**, 1172-1181, doi: 10.1016/j.enbuild.2010.02.008.

[102] Y. Hou, R. You, Investigating the impact of gaspers on airborne disease transmission in an economy-class aircraft cabin with personalized displacement ventilation, *Building and Environment*, 2023, **245**, 110963, doi: 10.1016/j.buildenv.2023.110963.

[103] Y. Hou, R. You, A practical concurrent gasper-operation strategy for controlling airborne disease transmission in an economy-class aircraft cabin with personalized displacement ventilation, *Building and Environment*, 2025, **285**, 113636, doi: 10.1016/j.buildenv.2025.113636.

[104] S. Liu, W. Wu, Z. Wang, H. Tian, J. Li, S. Ming, V. Vishnupriya, D. Dembele, X. Shen, Enhancing thermal-fluid dynamics in commercial aircraft cabins: energy-efficient pulsed ventilation strategies through CFD analysis, *Applied Thermal Engineering*, 2025, **279**, 127900, doi: 10.1016/j.applthermaleng.2025.127900.

[105] J. Bosbach, A. Heider, T. Dehne, M. Markwart, I. Gores, P. Bendfeldt, Evaluation of cabin displacement ventilation under flight conditions, *28th International Congress of the Aeronautical Sciences ICAS2012*, Brisbane Australia, 2012, **304**, 23-28.

[106] T. Zhang, Q. Chen, Novel air distribution systems for commercial aircraft cabins, *Building and Environment*, 2007, **42**, 1675-1684, doi: 10.1016/j.buildenv.2006.02.014.

[107] N. P. Gao, J. L. Niu, Personalized ventilation for commercial aircraft cabins, *Journal of Aircraft*, 2008, **45**, 508-512, doi: 10.2514/1.30272.

[108] P. Zítek, T. Vyhlídal, G. Simeunović, L. Nováková, J. Čížek, Novel personalized and humidified air supply for airliner passengers, *Building and Environment*, 2010, **45**, 2345-2353, doi: 10.1016/j.buildenv.2010.04.005.

[109] S. Liu, L. Xu, J. Chao, C. Shen, J. Liu, H. Sun, X. Xiao, G. Nan, Thermal environment around passengers in an aircraft cabin, *HVAC&R Research*, 2013, **19**, 627-634, doi: 10.1080/10789669.2013.803384.

[110] R. You, Investigating airflow distribution and contaminant transport in commercial aircraft cabins, Lafayette, USA, Purdue University, 2018.

[111] F. Wang, R. You, T. Zhang, Q. Chen, Recent progress on studies of airborne infectious disease transmission, air quality, and thermal comfort in the airliner cabin air environment, *Indoor Air*, 2022, **32**, e13032, doi: 10.1111/ina.13032.

[112] C. Giaconia, A. Orioli, A. Di Gangi, Air quality and relative humidity in commercial aircrafts: an experimental investigation on short-haul domestic flights, *Building and Environment*, 2013, **67**, 69-81, doi: 10.1016/j.buildenv.2013.05.006.

[113] Z. Yu, G. Xiao, C. Zhang, Y. Gui, Y. Du, Numerical study of air distribution and evolution characteristics in airliner cabin, *Processes*, 2022, **10**, 2621, doi: 10.3390/pr10122621.

[114] C. Ahmed Mboreha, J. Sun, Y. Wang, Z. Sun, Y. Zhang, Investigation of thermal comfort on innovative personalized ventilation systems for aircraft cabins: a numerical study with computational fluid dynamics, *Thermal Science and Engineering Progress*, 2021, **26**, 101081, doi: 10.1016/j.tsep.2021.101081.

[115] K. N. Rhee, K. W. Kim, A 50 year review of basic and applied research in radiant heating and cooling systems for the built environment, *Building and Environment*, 2015, **91**, 166-190, doi: 10.1016/j.buildenv.2015.03.040.

[116] K. N. Rhee, B. W. Olesen, K. W. Kim, Ten questions about radiant heating and cooling systems, *Building and Environment*, 2017, **112**, 367-381, doi: 10.1016/j.buildenv.2016.11.030.

[117] J. Babiak, B.W. Olesen, D. Petras, REHVA Guidebook No 7: Low temperature heating and high temperature cooling, *Federation of European Heating and Air-conditioning Associations*, Brussels, 2009.

[118] C. Zhang, M. Pomianowski, P. K. Heiselberg, T. Yu, A review of integrated radiant heating/cooling with ventilation systems- Thermal comfort and indoor air quality, *Energy and*

Buildings, 2020, **223**, 110094, doi: 10.1016/j.enbuild.2020.110094.
[119] O. B. Kazanci. Low temperature heating and high temperature cooling in buildings. Lyngby, Denmark. Technical University of Denmark, 2016.
[120] B. W. Olesen, Radiant floor heating in theory and practice, *ASHRAE journal*, 2002, **44**, 19-26.
[121] X. Hao, G. Zhang, Y. Chen, S. Zou, D. J. Moschandreas, A combined system of chilled ceiling, displacement ventilation and desiccant dehumidification, *Building and Environment*, 2007, **42**, 3298-3308, doi: 10.1016/j.buildenv.2006.08.020.
[122] B. Lin, Z. Wang, H. Sun, Y. Zhu, Q. Ouyang, Evaluation and comparison of thermal comfort of convective and radiant heating terminals in office buildings, *Building and Environment*, 2016, **106**, 91-102, doi: 10.1016/j.buildenv.2016.06.015.
[123] G. Sastry, VAV vs. radiant: side-by-side comparison, *ASHRAE journal*, 2014, **56**, 16.
[124] Ł. Amanowicz, K. Ratajczak, E. Dudkiewicz, Recent advancements in ventilation systems used to decrease energy consumption in buildings: literature review, *Energies*, 2023, **16**, 1853, doi: 10.3390/en16041853.
[125] R. Chen, L. Fang, J. Liu, B. Herbig, V. Norrefeldt, F. Mayer, R. Fox, P. Wargocki, Cabin air quality on non-smoking commercial flights: a review of published data on airborne pollutants, *Indoor Air*, 2021, **31**, 926-957, doi: 10.1111/ina.12831.